

Iridium-catalyzed Csp³-H Activation for Mild and Selective Hydrogen Isotope Exchange

William J. Kerr,^{*,†} Richard J. Mudd,[†] Marc Reid,[†] Jens Atzrodt,[‡] and Volker Derdau[‡]

[†]Department of Pure & Applied Chemistry, WestCHEM, University of Strathclyde, Glasgow G1 1XL, Scotland, UK.

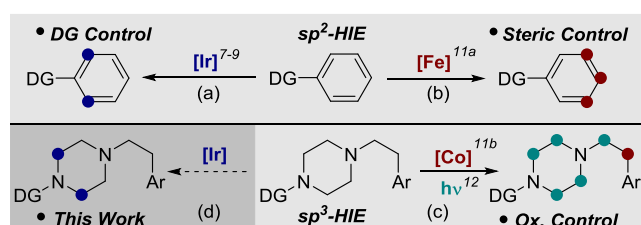
[‡]Integrated Drug Discovery, Isotope Chemistry, Sanofi-Aventis Deutschland GmbH, Industriepark Hoechst, Frankfurt, Germany.

ABSTRACT: The increasing demand for isotopically labeled compounds has provided appreciable impetus for the development of improved methods for the late stage introduction of isotopes of hydrogen (deuterium or tritium). Moreover, sp³-rich molecules are becoming increasingly common in the exploration of chemical space for drug design. Herein, we report an efficient iridium(I) catalyzed C-H activation method for the hydrogen isotope exchange of sp³ C-H bonds. A wide range of substrates have been labeled, including active pharmaceutical ingredients, delivering excellent levels of isotope incorporation and predictable regiocontrol, with low catalyst loadings, in short reaction times, and under mild reaction conditions.

KEYWORDS: C-H activation, iridium, isotopes, homogeneous catalysis, heterocycles.

Transition metal-mediated C-H activation has received significant attention in recent years, and continues to produce prominent new methods for complex chemical synthesis.¹ Despite such widespread use, the majority of applications are aimed towards sp² C-H bonds, which are intrinsically more readily activated, with considerably fewer applications targeting the activation of sp³ C-H bonds. Furthermore, iridium-catalyzed sp³ C-H activation processes are rare,^{10,2,3} with reported catalytic applications focused upon alkylation,^{3a,e} alkenylation,^{3b,c} oxidation,^{3d} and amidation.^{3f} However, in the majority of these cases, high temperatures and extended reaction times are required. In relation to this, hydrogen isotope exchange (HIE) provides a fundamental basis for the investigation of new C-H activation processes, as well as providing a means of generating valuable, specifically deuterated molecular units for mechanistic studies.⁴ Additionally, such flexible and direct methods of producing isotopically-labeled compounds are of appreciable importance for the pharmaceutical industry, especially within absorption, distribution metabolism, excretion, toxicity, and stability (ADMETs) studies of active pharmaceutical ingredients (APIs).^{4a,5}

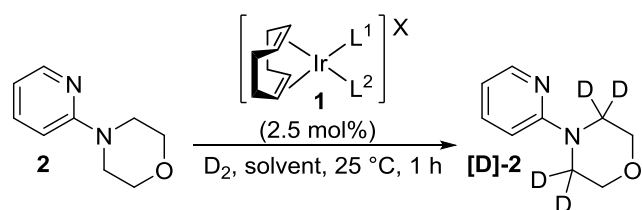
Inspired by the structural architecture of Crabtree's catalyst,^{6,7} we developed a series of iridium(I) complexes of the type [(COD)Ir(IMes)(PR₃)]X, capable of delivering heavy isotopes of hydrogen (deuterium, D, and tritium, T) to aromatic and olefinic compounds via a directed sp² C-H activation process, under mild conditions and short reaction times with a plethora of directing groups (Scheme 1, (a)).⁸⁻¹⁰ Complementary to the directing group approach, the growing interest in this area of research is further exemplified by recent reports detailing iron,^{11a} cobalt,^{11b} and photoredox¹² catalysis methods for the introduction of an isotopic label at sterically unencumbered aryl (sp²) and oxidatively active alkyl (sp³) positions, respectively (Scheme 1 (b) and (c)). Accordingly, a general method for the directed introduction of a hydrogen isotope at sp³ centers would deliver this previously unmet requirement, whilst also having the potential to provide further insight into sp³ C-H activation processes. Following the recent



Scheme 1. Complementary approaches to hydrogen isotope exchange.

disclosure of methylene labelling in a range of amides,^{3g} we now report the selective C-H activation and hydrogen isotope exchange on sp³ centers utilizing our developed iridium(I) NHC/phosphine complexes as directed by a range of pharmaceutically-relevant heterocyclic units, in turn expanding the utility of these catalysts and providing expedient access to a new range of important labeled chemical entities (Scheme 1 (d)).

Our studies commenced with the application of a range of developed iridium(I) complexes **1a-1e**, as well as Crabtree's catalyst **1f** and related BAR^F analogue **1g**, in a HIE reaction using commercially available 4-(pyridine-2-yl)morpholine **2**, as a typical, drug-like heterocyclic motif.¹³ Pleasingly, when applying the NHC/phosphine complex **1a**, we observed selective D-incorporation at the four positions α to the morpholine nitrogen only (Table 1, Entry 1). This incorporation was improved to deliver excellent levels of labeling by utilizing complex **1b** bearing the less coordinating BAR^F counterion (Table 1, Entry 2).^{8e,h,j} Further manipulation of the iridium complex by variation of the phosphine ligand resulted in a small decrease in D-incorporation (Table 1, Entries 3 and 4). Also, despite its reported use in sp² HIE,^{9a-c} the neutral complex **1e** proved to be inactive for sp³ exchange under these conditions (Table 1, Entry 5). Similarly, the smaller ligand sphere of Crabtree catalysts **1f** and **1g** delivered only low levels of D-incorporation (Table 1, Entries 6 and 7). With catalyst **1b** selected for further exploration of reaction parameters, we

Table 1. Screening of Catalysts 1a-g.^a

Entry	L ¹ , L ² , X ^b	Catalyst	Solvent	%D ^c
1	IMes, PPh ₃ , PF ₆	1a	DCM	79
2	IMes, PPh ₃ , BAR ^F	1b	DCM	90
3	IMes, PBn ₃ , BAR ^F	1c	DCM	85
4	IMes, PMePh ₂ , BAR ^F	1d	DCM	78
5	IMes, Cl	1e	DCM	0
6	Py, PCy ₃ , PF ₆	1f	DCM	24
7	Py, PCy ₃ , BAR ^F	1g	DCM	26
8	IMes, PPh ₃ , BAR ^F	1b	<i>t</i> AmylOH	76
9	IMes, PPh ₃ , BAR ^F	1b	MTBE	87
10	IMes, PPh ₃ , BAR ^F	1b	<i>t</i> BuOAc	86

^aEach entry displayed is the average of two reaction runs. Conditions: **2** (0.086 mmol), solvent (1 mL), catalyst (0.00215 mmol). ^bBAR^F = tetrakis(3,5-trifluoromethylphenyl)borate. ^cPercentage deuterium incorporation calculated from LCMS, with the position confirmed by ¹H NMR spectroscopy.

examined the flexibility of the reaction medium, understanding that many APIs are not soluble in DCM. Encouragingly, the reaction could be performed in a range of alcohol, ether and ester-derived solvents, with only a slight reduction in D-incorporation when applying *t*-amyl alcohol, MTBE or *t*-BuOAc (Table 1, Entries 8-10) (see ESI for full range of solvents tested).

Subsequent investigations examined the reaction conditions thoroughly, applying a design of experiments (DoE) approach¹⁴ to optimization of the labelling process using catalyst **1b** with substrate **2** in DCM. To this end, we applied a three-factor, two-level, full factorial design investigating the catalyst loading, reaction time, and reaction volume (see ESI for full details). This study clearly demonstrated that catalyst loading, and to a lesser extent reaction time, influenced the D-incorporation. Additionally, increasing the reaction volume was found to have a small positive effect upon the result, indicating that substrate complexation and subsequent product decomplexation influences the catalyst turnover,¹⁵ in accordance with our mechanistic observations in sp²-HIE systems.^{8d}

Following a detailed examination of the results garnered from the DoE, an optimized protocol using notably low catalyst loadings for sp³ C-H activation and HIE was developed (Scheme 2, Conditions A: **1b** (1 mol%), D₂, DCM (1 mL), 1

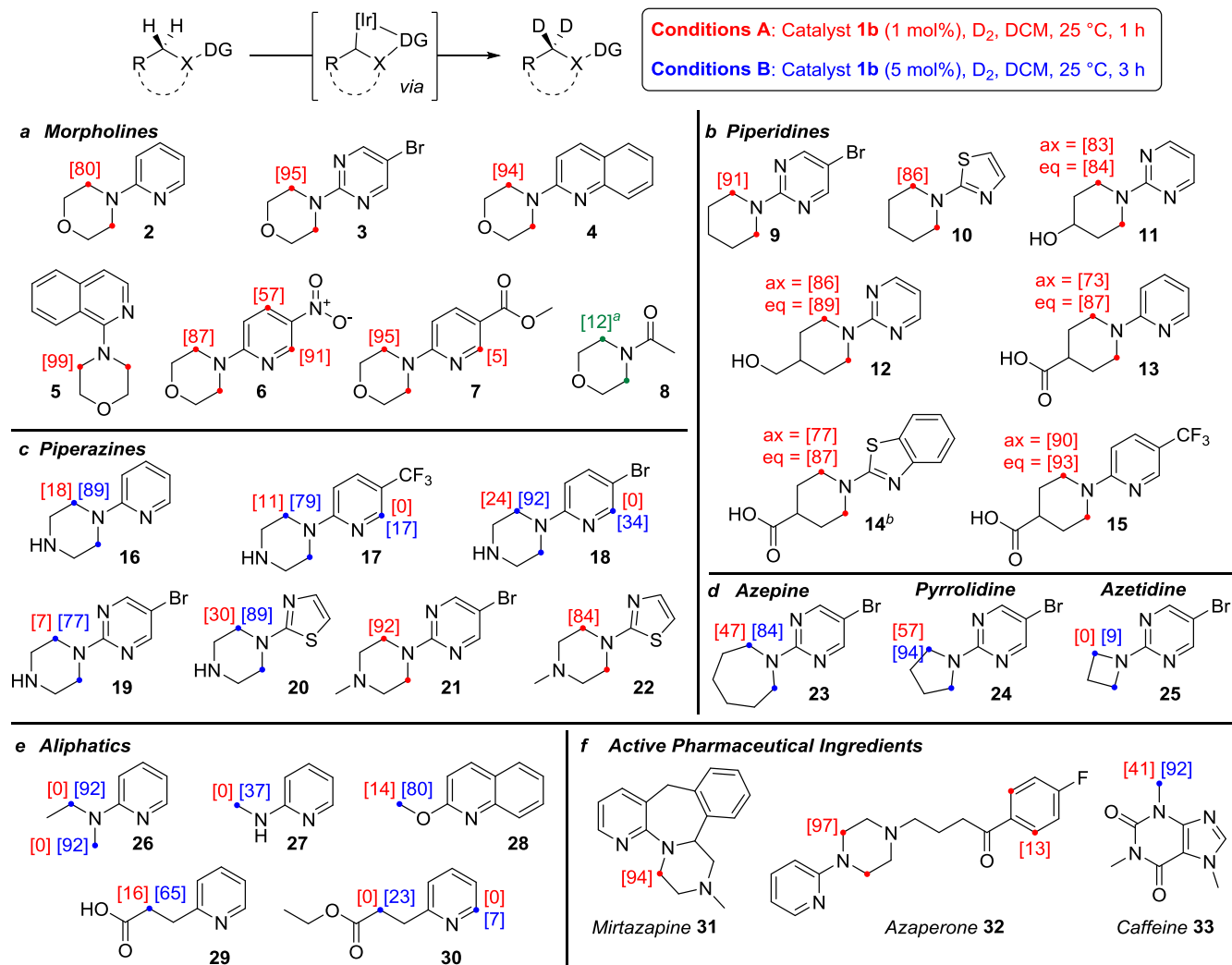
h), and applied to a range of saturated heterocyclic substrates (Scheme 2a). Initial studies focused on the influence that other *N*-heterocycles had when acting as a directing group for the C-H activation. Beyond previously applied pyridine substrate **2**, exchange was facilitated well with pyrimidine, quinoline, and isoquinoline directing groups, delivering ≥94% D-incorporation across the four specific C-H labeling sites of the morpholine ring in **3-5**. In addition to the sp³-exchange, D-incorporation was observed at positions *ortho* to the nitro and ester directing groups in **6** and **7**. Pleasingly, the sp³-exchange was preferred in the case of ester **7**, presumably because the greater Lewis basicity of the *N*-heterocyclic directing group favors coordination to the catalyst and subsequent sp³-exchange. This hypothesis is further supported by the example of *N*-acetyl morpholine **8**, where, under the optimized conditions, no D-incorporation was observed, and heating the reaction (5 mol% **1b**, D₂, MTBE, 50 °C, 3 h) resulted in only minimal incorporation.

Similar trends were observed within piperidine-derived substrates **9** and **11-15**, with consistently high D-incorporation being obtained (Scheme 2b). The level of labeling with thiazole **10** remained high despite the anticipated increase in ring strain present in the cyclometallated intermediate with this 5-membered directing heterocycle. Notably, compound **14** is insoluble in DCM, but the broad solvent compatibility of catalyst **1b** allowed this substrate to be labeled in 2-MeTHF, resulting in good levels of D-incorporation. In addition, where the axial and equatorial protons can be distinguished by ¹H NMR spectroscopy (**11-15**), the equatorial exchange is favored slightly, plausibly indicating a stronger agostic interaction between the catalyst and the equatorial C-H bond.

Following successful application to a range of morpholines and piperidines, we applied optimized Conditions A to piperazines (Scheme 2c), with initial results yielding lowered levels of D-incorporation (Conditions A, **16-20**). However, we observed that when the free amine was converted to an *N*-methyl unit, high incorporations were re-established (**19** vs **21**, and **20** vs **22**). Therefore, the decreased activity of these compounds clearly relates to an interaction between the free amine and catalyst, generating a different species from the active catalyst, as has been observed by ³¹P NMR spectroscopy (see ESI for full details).¹⁶ However, since the exchange process still continues, albeit to a lesser degree, the unreactive complex is presumed to form reversibly.

With this information in hand, we applied a second DoE phase, this time utilizing 1-(pyridin-2-yl)piperazine **16** as a reference substrate, to develop conditions that would facilitate exchange without protection of the piperazine. This DoE approach returned a similar dependency upon catalyst loading, reaction time, and reaction volume (see ESI for full details), and provided a second protocol (Conditions B: 5 mol% **1b**, D₂, DCM (1 mL), 3 h). Pleasingly, under the newly developed conditions, high levels of D-incorporation were observed and, crucially, without protection of piperazines **16-20**.

Keen to develop a general protocol for the labeling of saturated *N*-heterocycles, we next considered the effect of changing the size of the ring being labeled (Scheme 2d). Under Conditions A, HIE occurs to deliver a moderate D-incorporation within both azepane **23** and pyrrolidine **24**, but with no incorporation in azetidine **25**. In contrast, by utilizing Conditions B, high levels of D-incorporation can be achieved



Scheme 2. Hydrogen isotope exchange on saturated *N*-heterocycles. Conditions A or B with substrate (0.086 mmol) in DCM (1 mL). Percentage deuterium incorporation at each site calculated by ¹H NMR spectroscopy. ^a1b (5 mol%), MTBE, 50 °C, 3 h. ^bReaction performed in 2-MeTHF instead of DCM.

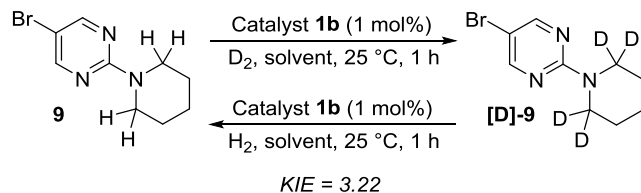
in **23** and **24**, and a small level of labelling is evolved in **25**. This series indicates that the heterocycle ring size can affect the efficiency of the HIE process, presumably by influencing the strain in the metallacyclic intermediate following C-H activation.

Following our success with saturated heterocycles, we next turned our attention to non-cyclic substrate components (Scheme 2e). Initial reactions with *N*-ethyl-*N*-methylpyridin-2-amine **26** and *N*-methylpyridin-2-amine **27** delivered no incorporation, and *O*-methylquinoline **28** showed only low levels of exchange on the *O*-methyl group. Accordingly, we turned to our second protocol, Conditions B, which gave high levels of incorporation at both the methyl- and methylene positions of **26**, and the *O*-methyl of **28**. In contrast, substrate **27** underwent only moderate levels of exchange, perhaps due to the unprotected secondary amine. Next, we examined several substrates with sp³ C-H bonds which do not possess an α -heteroatom, but which instead are adjacent to acid and ester functionalities (**29-30**). Under Conditions B, somewhat more moderate levels of D-incorporation were observed at the site arising from C-H activation via a 5-membered metallacycle.

Having established the utility of our labelling process on a broad range of heterocycles and acyclic substrates, we applied the developed method to several commercially available drug compounds (Scheme 2f). The anti-depressant *Mirtazapine* **31** does not contain any sp² centers which could be labelled via directed HIE, however its pyridine nitrogen could direct sp³ labelling. Applying conditions A, we were pleased to observe a high D-incorporation of 94% on the piperazine ring. Similarly, a high incorporation was obtained on the piperazine ring of the tranquilizer *Azaperone* **32**, and notably with excellent selectivity versus the *ortho* sp²-exchange directed by the ketone. Finally, application of conditions B to the stimulant *Caffeine* **33** resulted in a highly selective labelling at the 7-methyl position, directed by the imidazole nitrogen.

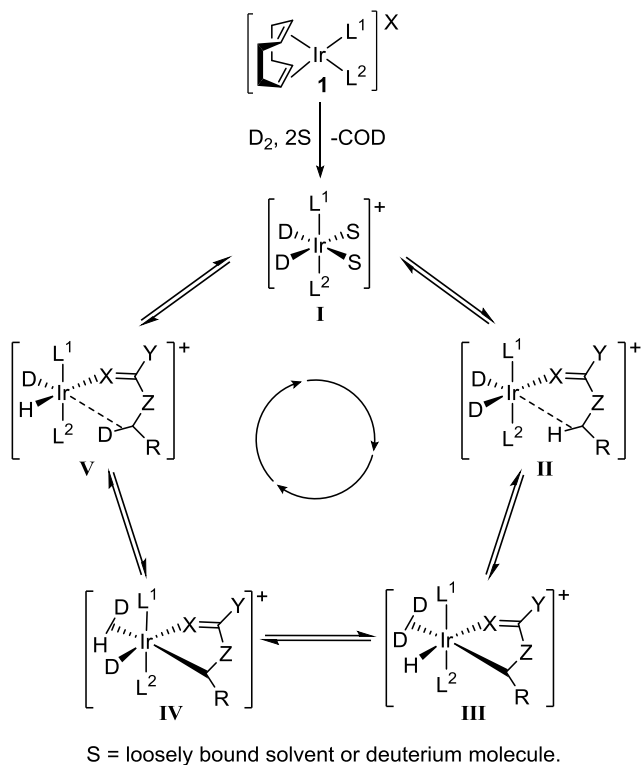
We next looked to investigate the mechanism through which the exchange occurs. Firstly, we confirmed a homogeneous catalysis process by continuation of the reaction in the presence of metallic mercury.¹⁷ Secondly, a mechanism involving more than one molecule of catalyst during the rate determining step was discounted, by observing a first order rate dependence with respect to catalyst (see ESI for full details). Finally, by measuring the rate of reaction for both the

installation and removal of deuterium (Scheme 3), a kinetic isotope effect of 3.22 was established, which indicates an iridium-mediated C-H activation as the rate determining step.¹⁸



Scheme 3. Kinetic isotope studies.

Taken together, these pieces of experimental evidence are consistent with our mechanistic observations in the sp^2 C-H activation and hydrogen isotope exchange catalyzed by complexes of type **1a-e**.^{8d,9b} As a result, it is plausible to propose a similar mechanistic pathway (Scheme 4), beginning with activation of the pre-catalyst **1** to the key iridium(III) dihydride intermediate **I**. Displacement of solvent and coordination of substrate, including the key agostic interaction with the exchange site, delivers **II**. Subsequent C-H insertion results in metallacycle **III**, followed by deuterium-hydrogen fluxionality affording complex **IV**. This intermediate can then undergo C-D bond formation to generate **V**, prior to product decomplexation and regeneration of active intermediate **I**.



Scheme 4. Proposed mechanism for sp^3 -hydrogen isotope exchange.

To conclude, we have developed new protocols for directed and selective hydrogen isotope exchange at sp^3 C-H centers, resulting in high levels of D-incorporation with low catalyst loadings and under mild reaction conditions. Exploration of a broad variety of substrates has shown the protocols to be efficient and reliable across a wide range of saturated het-

erocycles and aliphatic units. Application of the labelling conditions to commercial drug compounds also results in high levels of exchange selective for sp^3 positions. Beyond the substrate scope, we have investigated the mechanism of this process, providing evidence for a pathway proceeding *via* sp^3 -C-H activation as the rate determining step. Further work is underway in our laboratory to further explore the sp^3 -HIE of complex molecules and these studies will be reported in due course.

AUTHOR INFORMATION

Corresponding Author

*Email: w.kerr@strath.ac.uk

Notes

The authors declare no competing financial interest.

ASSOCIATED CONTENT

Details of experimental procedures and computational methods can be found in the Electronic Supporting Information (ESI). This material is available free of charge via the Internet at <http://pubs.acs.org>.

ACKNOWLEDGMENTS

Studentship (R.J.M.) support from the University of Strathclyde is gratefully acknowledged. W.J.K. and M.R. would like to thank the Carnegie Trust for funding. Mass spectrometry data were acquired at the EPSRC UK National Mass Spectrometry Facility at Swansea University.

REFERENCES

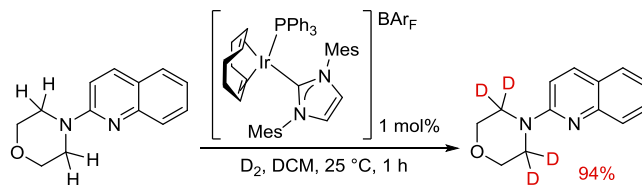
- (1) (a) Ackermann, L. Carboxylate-Assisted Transition-Metal-Catalyzed C-H Bond Functionalizations: Mechanism and Scope. *Chem. Rev.* **2011**, *111*, 1315-1345. (b) Wencel-Delord, J.; Dröge, T.; Liu, F.; Glorius, F. Towards Mild Metal-Catalyzed C-H Bond Activation. *Chem. Soc. Rev.* **2011**, *40*, 4740-4761. (c) Cho, S. H.; Kim, J. Y.; Kwak, J.; Chang, S. Recent Advances in the Transition Metal-Catalyzed Twofold Oxidative C-H Bond Activation Strategy for C-C and C-N Bond Formation. *Chem. Soc. Rev.* **2011**, *40*, 5068-5083. (d) Yeung, C. S.; Dong, V. M. Catalytic Dehydrogenative Cross-Coupling: Forming Carbon-Carbon Bonds by Oxidizing Two Carbon-Hydrogen Bonds. *Chem. Rev.* **2011**, *111*, 1215-1292. (e) McMurray, L.; O'Hara, F.; Gaunt, M. J. Recent Developments in Natural Product Synthesis using Metal-Catalysed C-H Bond Functionalisation. *Chem. Soc. Rev.* **2011**, *40*, 1885-1898. (f) Engle, K. M.; Mei, T.-S.; Wasa, M.; Yu, J.-Q. Weak Coordination as a Powerful Means for Developing Broadly Useful C-H Functionalization Reactions. *Acc. Chem. Res.* **2012**, *45*, 788-802. (g) Song, G.; Wang, F.; Li, X. C-C, C-O and C-N Bond Formation via Rhodium(III)-Catalyzed Oxidative C-H Activation. *Chem. Soc. Rev.* **2012**, *41*, 3651-3678. (h) Kuhl, N.; Hopkinson, M. N.; Wencel-Delord, J.; Glorius, F. Beyond Directing Groups: Transition-Metal-Catalyzed C-H Activation of Simple Arenes. *Angew. Chem. Int. Ed.* **2012**, *51*, 10236-10254. (i) Neufeldt, S. R.; Sanford, M. S. Controlling Site Selectivity in Palladium-Catalyzed C-H Bond Functionalization. *Acc. Chem. Res.* **2012**, *45*, 936-946. (j) Yamaguchi, J.; Yamaguchi, A. D.; Itami, K. C-H Bond Functionalization: Emerging Synthetic Tools for Natural Products and Pharmaceuticals. *Angew. Chem. Int. Ed.* **2012**, *51*, 8960-9009. (k) Shi, G.; Zhang, Y. Carboxylate-Directed C-H Functionalization. *Adv. Synth. Catal.* **2014**, *356*, 1419-1442. (l) Kuhl, N.; Schröder, N.; Glorius, F. Formal S_N -Type Reactions in Rhodium(III)-Catalyzed C-H Bond Activation. *Adv. Synth. Catal.* **2014**, *356*, 1443-1460. (m) De Sarkar, S.; Liu, W.; Kozhushkov, S. I.; Ackermann, L. Weakly Coordinating Directing Groups for Ruthenium(II)-Catalyzed C-H Activation. *Adv. Synth. Catal.* **2014**, *356*, 1461-1479. (n) Ackermann, L. Carboxylate-Assisted Ruthenium-Catalyzed Alkyne Annulations

- by C–H/Het–H Bond Functionalizations. *Acc. Chem. Res.* **2014**, *47*, 281–295. (o) Ros, A.; Fernández, R.; Lassaletta, J. M. Functional Group Directed C–H Borylation. *Chem. Soc. Rev.* **2014**, *43*, 3229–3243. (p) Girard, S. A.; Knauber, T.; Li, C.-J. The Cross-Dehydrogenative Coupling of C_{sp³}-H Bonds: A Versatile Strategy for C–C Bond Formations. *Angew. Chem. Int. Ed.* **2014**, *53*, 74–100. (q) Yang, L.; Huang, H. Transition-Metal-Catalyzed Direct Addition of Unactivated C–H Bonds to Polar Unsaturated Bonds. *Chem. Rev.* **2015**, *115*, 3468–3517. (r) Xue, X.-S.; Ji, P.; Zhou, B.; Cheng, J.-P. The Essential Role of Bond Energetics in C–H Activation/Functionalization. *Chem. Rev.* **2017**, *117*, 8622–8648. (s) Newton, C. G.; Wang, S.-G.; Oliveira, C. C.; Cramer, N. Catalytic Enantioselective Transformations Involving C–H Bond Cleavage by Transition-Metal Complexes. *Chem. Rev.* **2017**, *117*, 8908–8976. (t) Qin, Y.; Zhu, L.; Luo, S. Organocatalysis in Inert C–H Bond Functionalization. *Chem. Rev.* **2017**, *117*, 9433–9520.
- (2) For selected stoichiometric examples of iridium-catalyzed sp³-C–H activation, see: (a) Janowicz, A. H.; Bergman, R. G. Carbon-Hydrogen Activation in Completely Saturated Hydrocarbons: Direct Observation of M + R–H → M(R)(H). *J. Am. Chem. Soc.* **1982**, *104*, 352–354. (b) Jiménez-Cataño, R.; Hall, M. B. Theoretical Studies of Inorganic and Organometallic Reaction Mechanisms. 9. Intermolecular versus Intramolecular Carbon–Hydrogen Bond Activation in Zirconium, Rhodium, and Iridium Complexes. *Organometallics* **1996**, *15*, 1889–1897. (c) Rodríguez, P.; Díaz-Requejo, M. M.; Belderrain, T. R.; Trofimenko, S.; Nicasio, M. C.; Pérez, P. J. Alkane Dehydrogenation by Sequential, Double C–H Bond Activation by Tp^{Br3}Ir(C₂H₄)₂ (Tp^{Br3} = hydrotris(3,4,5-tribromopyrazolyl)borate). *Organometallics* **2004**, *23*, 2162–2167. (d) Tanabe, Y.; Hanasaka, F.; Fujita, K.-I.; Yamaguchi, R. Scope and Mechanistic Studies of Intramolecular Aliphatic C–H Bond Activation of N-Heterocyclic Carbene Iridium Complexes. *Organometallics* **2007**, *26*, 4618–4626. (e) Cheung, C. W.; Chan, K. S. Scope and Mechanistic Studies of Intramolecular Aliphatic C–H Bond Activation of N-Heterocyclic Carbene Iridium Complexes. *Organometallics* **2008**, *27*, 3043–3055. (f) Conejero, S.; Paneque, M.; Poveda, M. L.; Santos, L. L.; Carmona, E. C–H Bond Activation Reactions of Ethers That Generate Iridium Carbenes. *Acc. Chem. Res.* **2010**, *43*, 572–580. (g) Ito, J.-I.; Kaneda, T.; Nishiyama, H. Intermolecular C–H Bond Activation of Alkanes and Arenes by NCN Pincer Iridium(III) Acetate Complexes Containing Bis(oxazolonyl)phenyl Ligands. *Organometallics* **2012**, *31*, 4442–4449. (h) Donnelly, K. F.; Lalrempuia, R.; Müller-Bunz, H.; Clot, E.; Albrecht, M. Controlling the Selectivity of C–H Activation in Pyridinium Triazolylidene Iridium Complexes: Mechanistic Details and Influence of Remote Substituents. *Organometallics* **2015**, *34*, 858–869.
- (3) For selected sub-stoichiometric examples of iridium-catalysed sp³-C–H activation, see: (a) Yingrui, L.; Dawei, M.; Xiyan, L. Iridium Pentahydride Complex Catalyzed Formation of C–C Bond By C–H Bond Activation Followed by Olefin Insertion. *Tetrahedron Lett.* **1987**, *28*, 3249–3252. (b) DeBoef, B.; Pastine, S. J.; Sames, D. Cross-Coupling of sp³ C–H Bonds and Alkenes: Catalytic Cyclization of Alkene–Amide Substrates. *J. Am. Chem. Soc.* **2004**, *126*, 6556–6557. (c) Tsuchikama, K.; Kasagawa, M.; Endo, K.; Shibata, T. Cationic Ir(I)-Catalyzed sp³ C–H Bond Alkenylation of Amides with Alkynes. *Org. Lett.* **2009**, *11*, 1821–1823. (d) Zhou, M.; Schley, N. D.; Crabtree, R. H. Cp* Iridium Complexes Give Catalytic Alkane Hydroxylation with Retention of Stereochemistry. *J. Am. Chem. Soc.* **2010**, *132*, 12550–12551. (e) Pan, S.; Endo, K.; Shibata, T. Ir(I)-Catalyzed Enantioselective Secondary sp³ C–H Bond Activation of 2-(Alkylamino)pyridines with Alkenes. *Org. Lett.* **2011**, *13*, 4692–4695. (f) Kang, T.; Kim, Y.; Lee, D.; Wang, Z.; Chang, S. Iridium-Catalyzed Intermolecular Amidation of sp³ C–H Bonds: Late-Stage Functionalization of an Unactivated Methyl Group. *J. Am. Chem. Soc.* **2014**, *136*, 4141–4144. (g) Valero, M.; Weck, R.; Güssregen, S.; Atzrodt, J.; Derdau, V. Highly Selective Directed Iridium-Catalyzed Hydrogen Isotope Exchange Reactions of Aliphatic Amides. *Angew. Chem. Int. Ed.* **2018**, *57*, 8159–8163.
- (4) For recent reviews on hydrogen isotope exchange processes, see: (a) Atzrodt, J.; Derdau, V.; Fey, T.; Zimmermann, J. The Renaissance of H/D Exchange. *Angew. Chem. Int. Ed.* **2007**, *46*, 7744–7765. (b) Heys, J. R. Organoiridium Complexes for Hydrogen Isotope Exchange Labeling. *J. Labelled Compd. Radiopharm.* **2007**, *50*, 770–778. (c) Lockley, W. J. S. Hydrogen Isotope Labelling Using Iridium(I) Dionates. *J. Labelled Compd. Radiopharm.* **2010**, *53*, 668–673. (d) Salter, R. The Development and Use of Iridium(I) Phosphine Systems for ortho-Directed Hydrogen-Isotope Exchange. *J. Labelled Compd. Radiopharm.* **2010**, *53*, 645–657. (e) Allen, P. H.; Hickey, M. J. L.; Kingston, P.; Wilkinson, D. J. Metal-Catalysed Isotopic Exchange Labelling: 30 Years of Experience in Pharmaceutical R&D. *J. Labelled Compd. Radiopharm.* **2010**, *53*, 731–738. (f) Atzrodt, J.; Derdau, V.; Kerr, W. J.; Reid, M. C–H Functionalisation for Hydrogen Isotope Exchange. *Angew. Chem. Int. Ed.* **2018**, *57*, 3022–3047.
- (5) (a) Lockley, W. J. S. 30 Years with ortho-Directed Hydrogen Isotope Exchange Labelling. *J. Labelled Compd. Radiopharm.* **2007**, *50*, 779–788. (b) Isin, E. M.; Elmore, C. S.; Nilsson, G. N.; Thompson, R. A.; Weidolf, L. Use of Radiolabeled Compounds in Drug Metabolism and Pharmacokinetic Studies. *Chem. Res. Toxicol.* **2012**, *25*, 532–542. (c) Lockley, W. J. S.; McEwen, A.; Cooke, R. Tritium: A Coming of Age for Drug Discovery and Development ADME Studies. *J. Labelled Compd. Radiopharm.* **2012**, *55*, 235–257. (d) Atzrodt, J.; Derdau, V.; Kerr, W. J.; Reid, M. Deuterium- and Tritium-Labelled Compounds: Applications in the Life Sciences. *Angew. Chem. Int. Ed.* **2018**, *57*, 1758–1784.
- (6) (a) Crabtree, R. H.; Felkin, H.; Morris, G. E. Cationic Iridium Diolefin Complexes as Alkene Hydrogenation Catalysts and the Isolation of Some Related Hydrido Complexes. *J. Organomet. Chem.* **1977**, *141*, 205–215. (b) Crabtree, R. H. Iridium Compounds in Catalysis. *Acc. Chem. Res.* **1979**, *12*, 331–337.
- (7) For applications of Crabtree's catalyst in hydrogen isotope exchange see: (a) Hesk, D.; Das, P. R.; Evans, B. Deuteration of Acetanilides and Other Substituted Aromatics Using [Ir(COD)(C₃P)(Py)]PF₆ as Catalyst. *J. Labelled Compd. Radiopharm.* **1995**, *36*, 497–502. (b) Ellames, G. J.; Gibson, J. S.; Herbert, J. M.; McNeill, A. H. The Scope and Limitations of Deuteration Mediated by Crabtree's Catalyst. *Tetrahedron* **2001**, *57*, 9487–9497. (c) Bushby, N.; Killick, D. A. Hydrogen Isotope Exchange at Alkyl Positions Using Crabtree's Catalyst and its Application to the Tritiation of Methapyrilene. *J. Labelled Compd. Radiopharm.* **2007**, *50*, 519–520. (d) Schou, S. C. The Effect of Adding Crabtree's Catalyst to Rhodium Black in Direct Hydrogen Isotope Exchange Reactions. *J. Labelled Compd. Radiopharm.* **2009**, *52*, 376–381. (e) Hesk, D.; Lavey, C. F.; McNamara, P. Tritium Labelling of Pharmaceuticals by Metal-Catalysed Exchange Methods. *J. Labelled Compd. Radiopharm.* **2010**, *53*, 722–730. (f) Vliegen, M.; Haspelslagh, P.; Verluyten, W. Alternative Efficient Tritium Labeling of Repaglinide. *J. Labelled Compd. Radiopharm.* **2012**, *55*, 155–157.
- (8) (a) Brown, J. A.; Irvine, S.; Kennedy, A. R.; Kerr, W. J.; Andersson, S.; Nilsson, G. N. Highly Active Iridium(I) Complexes for Catalytic Hydrogen Isotope Exchange. *Chem. Commun.* **2008**, 1115–1117. (b) Nilsson, G. N.; Kerr, W. J. The Development and Use of Novel Iridium Complexes as Catalysts for ortho-Directed Hydrogen Isotope Exchange Reactions. *J. Labelled Compd. Radiopharm.* **2010**, *53*, 662–667. (c) Cochrane, A. R.; Idziak, C.; Kerr, W. J.; Mondal, B.; Paterson, L. C.; Tuttle, T.; Andersson, S.; Nilsson, G. N. Practically Convenient and Industrially-Aligned Methods for Iridium-Catalysed Hydrogen Isotope Exchange Processes. *Org. Biomol. Chem.* **2014**, *12*, 3598–3603. (d) Brown, J. A.; Cochrane, A. R.; Irvine, S.; Kerr, W. J.; Mondal, B.; Parkinson, J. A.; Paterson, L. C.; Reid, M.; Tuttle, T.; Andersson, S.; Nilsson, G. N. The Synthesis of Highly Active Iridium(I) Complexes and Their Application in Catalytic Hydrogen Isotope Exchange. *Adv. Synth. Catal.* **2014**, *356*, 3551–3562. (e) Kennedy, A. R.; Kerr, W. J.; Moir, R.; Reid, M. Anion Effects to Deliver Enhanced Iridium Catalysts for Hydrogen Isotope Exchange Processes. *Org. Biomol. Chem.* **2014**, *12*, 7927–7931. (f) Kerr, W. J.; Mudd, R. J.; Paterson, L. C.; Brown, J. A. Iridium(I)-Catalyzed Regioselective C–H Activation and Hydrogen-Isotope Exchange of Non-Aromatic Unsaturated Functionality. *Chem. Eur. J.* **2014**, *20*, 14604–14607. (g) Atzrodt, J.; Derdau, V.; Kerr, W. J.; Reid, M.; Rojahn, P.; Weck, R. Expanded Applicability of Iridium(I) NHC/Phosphine Catalysts in Hydrogen Isotope Exchange Processes with Pharmaceutically-Relevant Heterocycles. *Tetrahedron* **2015**, *71*, 1924–1929. (h) Devlin,

- J.; Kerr, W. J.; Lindsay, D. M.; McCabe, T. J. D.; Reid, M.; Tuttle, T. Iridium-Catalysed Ortho-Directed Deuterium Labelling of Aromatic Esters—An Experimental and Theoretical Study on Directing Group Chemoselectivity. *Molecules* **2015**, *20*, 11676-11698. (i) Kerr, W. J.; Lindsay, D. M.; Reid, M.; Atzrodt, J.; Derdau, V.; Rojahn, P.; Weck, R. Iridium-Catalysed Ortho-H/D and -H/T Exchange under Basic Conditions: C–H Activation of Unprotected Tetrazoles. *Chem. Commun.* **2016**, *52*, 6669-6672. (j) Kerr, W. J.; Mudd, R. J.; Owens, P. K.; Reid, M.; Brown, J. A.; Campos, S. Hydrogen Isotope Exchange with Highly Active Iridium(I) NHC/Phosphine Complexes: A Comparative Counterion Study. *J. Labelled Compd. Radiopharm.* **2016**, *59*, 601-603. (k) Kerr, W. J.; Lindsay, D. M.; Owens, P. K.; Reid, M.; Tuttle, T.; Campos, S. Site-Selective Deuteration of N-Heterocycles via Iridium-Catalyzed Hydrogen Isotope Exchange. *ACS Catal.* **2017**, *7*, 7182-7186.
- (9) For the use of complexes of the type [(COD)Ir(NHC)Cl] in HIE processes, see: (a) Cochrane, A. R.; Irvine, S.; Kerr, W. J.; Reid, M.; Andersson, S.; Nilsson, G. N. Application of Neutral Iridium(I) N-Heterocyclic Carbene Complexes in ortho-Directed Hydrogen Isotope Exchange. *J. Labelled Compd. Radiopharm.* **2013**, *56*, 451-454. (b) Kerr, W. J.; Reid, M.; Tuttle, T. Iridium-Catalyzed C–H Activation and Deuteration of Primary Sulfonamides: An Experimental and Computational Study. *ACS Catal.* **2015**, *5*, 402-410. (c) Burhop, A.; Weck, R.; Atzrodt, J.; Derdau, V. Hydrogen-Isotope Exchange (HIE) Reactions of Secondary and Tertiary Sulfonamides and Sulfonylureas with Iridium(I) Catalysts. *Eur. J. Org. Chem.* **2017**, *2017*, 1418-1424. (d) Kerr, W. J.; Reid, M.; Tuttle, T. Iridium-Catalyzed Formyl-Selective Deuteration of Aldehydes. *Angew. Chem. Int. Ed.* **2017**, *56*, 7808-7812.
- (10) These complexes also find application in olefin hydrogenation; see: (a) Bennie, L. S.; Fraser, C. J.; Irvine, S.; Kerr, W. J.; Andersson, S.; Nilsson, G. N. Highly Active Iridium(I) Complexes for the Selective Hydrogenation of Carbon–Carbon Multiple Bonds. *Chem. Commun.* **2011**, *47*, 11653-11655. (b) Kerr, W. J.; Mudd, R. J.; Brown, J. A. Iridium(I) N-Heterocyclic Carbene (NHC)/Phosphine Catalysts for Mild and Chemoselective Hydrogenation Processes. *Chem. Eur. J.* **2016**, *22*, 4738-4742.
- (11) (a) Yu, R. P.; Hesk, D.; Rivera, N.; Pelczar, I.; Chirik, P. J. Iron-Catalysed Tritiation of Pharmaceuticals. *Nature* **2016**, *529*, 195-199. (b) Palmer, W. N.; Chirik, P. J. Cobalt-Catalyzed Stereoretentive Hydrogen Isotope Exchange of C(sp³)–H Bonds. *ACS Catal.* **2017**, *7*, 5674-5678.
- (12) Loh, Y. Y.; Nagao, K.; Hoover, A. J.; Hesk, D.; Rivera, N. R.; Colletti, S. L.; Davies, I. W.; MacMillan, D. W. C. Photoredox-Catalyzed Deuteration and Tritiation of Pharmaceutical Compounds. *Science* **2017**, *358*, 1182-1187.
- (13) The chosen reference compound is common within drug design. For further details see: Vitaku, E.; Smith, D. T.; Njardarson, J. T. Analysis of the Structural Diversity, Substitution Patterns, and Frequency of Nitrogen Heterocycles among U.S. FDA Approved Pharmaceuticals. *J. Med. Chem.* **2014**, *57*, 10257-10274.
- (14) (a) Brereton, R. *Applied Chemometrics for Scientists*, 1st ed.; John Wiley & Sons Ltd: West Sussex, U.K. 2007, p 9. (b) Leardi, R. Experimental Design in Chemistry: A Tutorial. *Anal. Chim. Acta.* **2009**, *652*, 161-172.
- (15) For examples of substrate and product inhibition in similar catalytic systems, see: Heller, D.; de Vries, A. H. M.; de Vries, J. G. Catalyst Inhibition and Deactivation in Homogeneous Hydrogenation. In *Handbook of Homogeneous Hydrogenation*, 1st ed.; de Vries, J. G.; Elsevier, C. J., Eds.; Wiley-VCH: Weinheim, Germany 2007; pp 1494-1499.
- (16) For an example of iridium interacting with unprotected amines, see: Sykes, A. C.; White, P.; Brookhart, M. Reactions of Anilines and Benzamides with a 14-Electron Iridium(I) Bis(phosphinite) Complex: N–H Oxidative Addition versus Lewis Base Coordination. *Organometallics* **2006**, *25*, 1664-1675.
- (17) Whitesides, G. M.; Hackett, M.; Brainard, R. L.; Lavalleye, J.-P. P. M.; Sowinski, A. F.; Izumi, A. N.; Moore, S. S.; Brown, D. W.; Staudt, E. M. Suppression of Unwanted Heterogeneous Platinum(0)-Catalyzed Reactions by Poisoning with Mercury(0) in Systems Involving Competing Homogeneous Reactions of Soluble Organoplati-
- num Compounds: Thermal Decomposition of Bis(Triethylphosphine)-3,3,4,4-Tetramethylplatinacyclopentane. *Organometallics* **1985**, *4*, 1819-1830.
- (18) (a) Gómez-Gallego, M.; Sierra, M. A. Kinetic Isotope Effects in the Study of Organometallic Reaction Mechanisms. *Chem. Rev.* **2011**, *111*, 4857-4963. (b) Jones, W. D. Isotope Effects in C–H Bond Activation Reactions by Transition Metals. *Acc. Chem. Res.* **2003**, *36*, 140-146.

SYNOPSIS TOC (Word Style "SN_Synopsis_TOC"). If you are submitting your paper to a journal that requires a synopsis graphic and/or synopsis paragraph, see the Instructions for Authors on the journal's homepage for a description of what needs to be provided and for the size requirements of the artwork.

Authors are required to submit a graphic entry for the Table of Contents (TOC) that, in conjunction with the manuscript title, should give the reader a representative idea of one of the following: A key structure, reaction, equation, concept, or theorem, etc., that is discussed in the manuscript. Consult the journal's Instructions for Authors for TOC graphic specifications.



- High deuterium incorporation (up to 99%)
- Mild reaction conditions
- >30 examples (including drug compounds)
- Selectivity over aromatic labeling

Supporting Information:

Iridium-catalyzed Csp³-H Activation for Mild and Selective Hydrogen Isotope Exchange

William J. Kerr,^{*,†} Richard J. Mudd,[†] Marc Reid,[†] Jens Atzrodt[‡] and Volker Derdau[‡]

[†]Department of Pure and Applied Chemistry, WestCHEM, University of Strathclyde, Glasgow, G1 1XL, Scotland, UK.

[‡]Integrated Drug Discovery, Isotope Chemistry, Sanofi-Aventis Deutschland GmbH, Industriepark Hoechst, Frankfurt, Germany

* w.kerr@strath.ac.uk

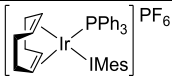
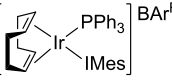
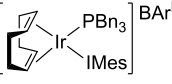
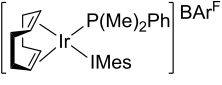
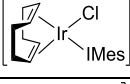
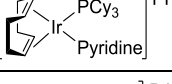
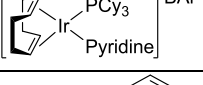
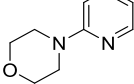
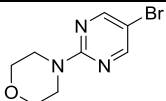
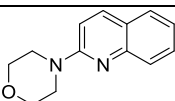
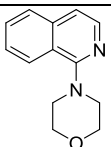
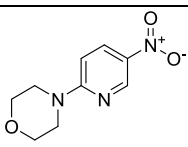
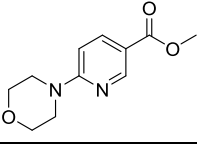
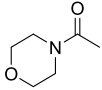
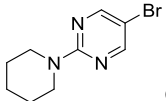
Contents

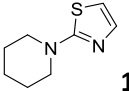
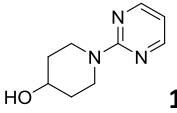
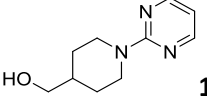
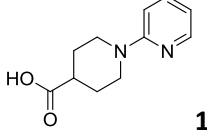
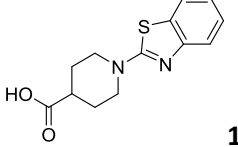
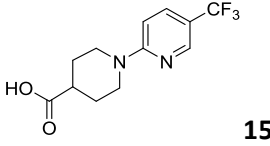
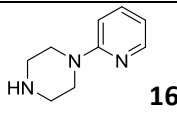
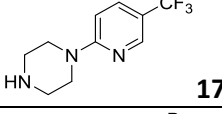
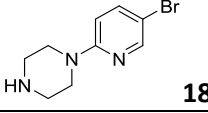
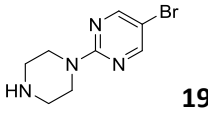
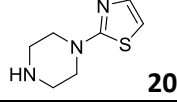
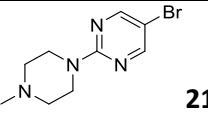
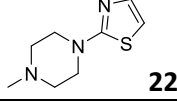
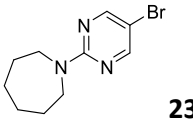
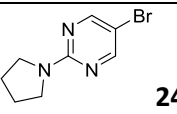
1. General experimental information	3
2. General procedure for exchange reactions using Heidolph synthesis 1 liquid 16 device.	7
3. Preparation of [(COD)Ir(IMes)(PBn ₃)]BARF 1c	8
4. Screening of Catalysts 1a-1g and Extended Solvent Screen (Manuscript Table 1).....	9
5. Design of Experiment.....	10
5.1. Optimisation for Conditions A.	10
5.2. Optimisation for Conditions B.....	12
6. Substrate Scope (Manuscript Scheme 2)	14
7. NMR Studies Regarding Piperazine NH Binding.....	25
8. Mechanistic Investigations.....	26
8.1. Mercury Nanoparticle Test	26
8.2. Order of Reaction.....	27
8.3. Kinetic Isotope Effect	28
9. Compound Spectra.....	29
9.1. Catalyst [(COD)Ir(IMes)(PBn ₃)]BARF, 1c	29
9.2. Example LC-MS and NMR data of unlabelled and labelled substrates (2 and [D]- 2)	34
10. References	35

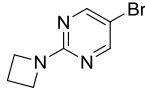
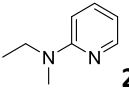
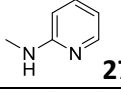
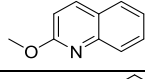
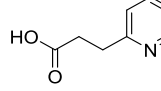
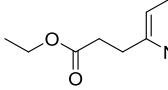
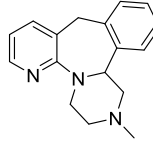
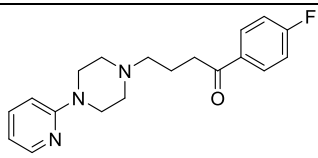
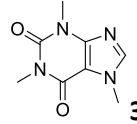
1. General experimental information

All reagents were obtained from commercial suppliers (**Table S1**) and used without further purification, unless otherwise stated. Purification was carried out according to standard laboratory methods.

Table S1. Starting materials and suppliers.

Entry	Structure	Supplier / Synthesis
1	 1a	Strem
2	 1b	Prepared according to reference [1]
3	 1c	See ESI page S8
4	 1d	Prepared according to reference [2]
5	 1e	Prepared according to reference [1]
6	 1f	Strem
7	 1g	Prepared according to reference [3]
8	 2	Sigma-Aldrich
9	 3	Combi-Blocks
10	 4	Sigma-Aldrich
11	 5	Sigma-Aldrich
12	 6	Alfa-Aesar
13	 7	Maybridge
14	 8	Sigma-Aldrich
15	 9	Fluorochem

16	 10	Fluorochem
17	 11	Synchem
18	 12	Maybridge
19	 13	Fluorochem
20	 14	Enamine
21	 15	Fluorochem
22	 16	Sigma-Aldrich
23	 17	Fluorochem
24	 18	Apollo Scientific
25	 19	ABCR
26	 20	Fluorochem
27	 21	Apollo Scientific
28	 22	Fluorochem
29	 23	Fluorochem
30	 24	Fluorochem

31	 25	Fluorochem
32	 26	TCI
33	 27	Sigma-Aldrich
34	 28	Combi-Blocks
35	 29	Fluorochem
36	 30	Fluorochem
37	 31	TCI
38	 32	Sigma-Aldrich
39	 33	ABCR
40	Sodium tetrakis[3,5-bis(trifluoromethyl)phenyl]borate (NaBARF)	Sigma Aldrich
41	Tribenzylphosphine (PBN ₃)	Sigma Aldrich

Hydrogen isotope exchange reactions were carried out on a Heidolph Synthesis 1 Liquid 16 device (**Figure S1**).



Figure S1. Heidolph synthesis 1 liquid 16 device.

¹H (300, 500 MHz) and ¹³C (75, 125 MHz) NMR spectra were obtained on Bruker spectrometers in the solvents indicated. Chemical shifts are reported in ppm. Coupling constants are reported in Hz and refer to ³J_{H-H} couplings,

unless otherwise stated. ^1H NMR spectra of labeled products were obtained using a 10 second delay to allow full relaxation of all hydrogen environments ($D1 = 10$).

IR spectra were obtained on a Shimadzu IRAffinity-1 Spectrophotometer machine and values are reported in cm^{-1} , unless stated otherwise.

Thin layer chromatography was carried out using Camlab silica plates coated with fluorescent indicator UV_{254} . The plates were analysed using a Mineralight UVGL-25 lamp or developed using vanillin or KMnO_4 solution.

Flash column chromatography was carried out using Prolabo silica gel (230-400 mesh).

Mass spectrometry data was acquired at the EPSRC UK National Mass Spectrometry Facility at Swansea University.

The distribution of hydrogen isotopes in the products was determined by a liquid chromatography-mass spectrometry (LC-MS) system with a Symmetry Shield RP18 column, 3.9 x 150 mm, with a gradient program. LC column conditions were as follows:

Mobile phase A: water (900 mL), acetonitrile (100 mL), TFA (1 mL)

Mobile phase B: water (100 mL), acetonitrile (900 mL), TFA (1 mL)

Gradient program: 0-4 min: 5% A/95% B

4-7 min: 10% A/90% B

Flow rate: 1.0 mL/min

Detection: UV 254 nm.

2. General procedure for exchange reactions using Heidolph synthesis 1 liquid 16 device.

The apparatus was evacuated then filled with argon, and the water condenser was turned on. To a carousel tube was added the substrate of choice (0.086 mmol), and iridium catalyst (0.00086 mmol (1 mol%) or 0.00215 mmol (2.5 mol%) or 0.0043 mmol (5 mol%)). The requisite solvent was then added, rinsing the inner walls of the tube. The tube was then sealed at the screw cap (with the gas inlet left open) under argon. The flask was then twice evacuated and refilled with deuterium *via* a balloon. The carousel gas inlet tube was then closed, creating a sealed atmosphere of deuterium, the carousel shaking motion was initiated (750 rpm) and the temperature set (25 °C unless otherwise stated). After starting the device, the timer was initiated and a rapid red/orange to clear/yellow colour change was observed. The reaction mixture was stirred for the allotted time (1 h or 3 h) before removing excess deuterium and replacing with air. The yellow solution was then prepared for analysis by LC-MS and ¹H NMR spectroscopy.

The level and regioselectivity of deuterium incorporation in the substrate was determined by ¹H NMR spectroscopy. The integrals were calibrated against a peak corresponding to a position not expected to be labelled. Equation 1 was then used to calculate the extent of labelling.

$$\% \text{ Deuteration} = 100 - \left[\left(\frac{\text{residual integral}}{\text{number of exchangeable sites}} \right) \times 100 \right]$$

Equation 1

For example, in a substrate containing four possible positions of exchange, the percentage given refers to the level of deuterium incorporation over the total number of positions (see page S34 for an example of such a spectrum).

The incorporation of deuterium into each substrate was verified by LC-MS, observing a shift in the isotope distribution in the starting material (M) to show M+1 (d₁), M+2 (d₂), M+3 (d₃), etc.

Example LC-MS analysis of compound 2:

~5 μL of the labelling reaction mixture was removed and diluted with 0.5 mL of MeCN, and the sample analysed by LC-MS. Data processing was performed using ADvion Mass express analysis software and the given formula:

# of D atoms incorporated	D0	D1	D2	D3	D4
Integral of MS peak	0	0.2	0.23	1.2	1.3
Percentage	0%	6.3%	15.6%	37.5%	40.6%

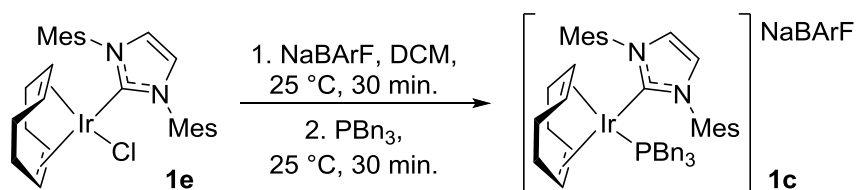
$$\text{Total incorporation} = (\%D1 \times 0.25) + (\%D2 \times 0.5) + (\%D3 \times 0.75) + (\%D4 \times 1)$$

$$\text{Total incorporation} = (6.3 \times 0.25) + (15.6 \times 0.5) + (37.5 \times 0.75) + (40.6 \times 1)$$

$$\text{Total incorporation} = (1.6) + (7.8) + (28.1) + (40.6) = 78.1\%$$

3. Preparation of [(COD)Ir(IMes)(PBN₃)]BARf **1c**

The catalyst was prepared according to a modified procedure from reference [1].



To a flame-dried, argon-cooled Schlenk tube was added IMes/chloride complex **1e**¹ (320 mg, 0.5 mmol, 1 eq), dry DCM (10 mL) and NaBAR^f (443 mg, 0.5 mmol, 1 eq). After stirring at 25 °C for 30 min, tribenzylphosphine (152 mg, 0.5 mmol, 1 eq) was added slowly, initiating an orange to red colour change. Following a further 30 min stirring, the solvent was removed *in vacuo* leaving a red oily solid. The residue was purified by flash column chromatography, eluting with DCM/petroleum ether 40-60 °C (50/50). The isolated catalyst was dried in a vacuum oven (40 °C, 1 mbar) for 24 h, yielding **1c** as a deep red solid (762 mg, 86% yield).

Melting Point (°C): >175 (dec).

FTIR (neat): (cm⁻¹): 2978, 2361, 1495.

¹H NMR (400 MHz, CDCl₃): δ 7.79 (8H, t ⁴J = 2.3 Hz, Ar-H), 7.58 (4H, s, Ar-H), 7.37-7.27 (13H, m, Ar-H), 7.25-7.21 (2H, m, Ar-H), 6.92-6.87 (6H, m, N-CH and Ar-H), 4.66-4.61 (2H, m, COD-CH), 3.31-3.27 (2H, m, COD-CH), 2.90 (6H, d ²J = 8.7 Hz, P-CH₂-Ar), 2.51 (6H, s, Ar-CH₃), 2.50 (6H, s, Ar-CH₃), 2.33 (6H, s, Ar-CH₃), 1.86-1.73 (2H, m, COD-CH₂), 1.65-1.49 (4H, m, COD-CH₂), 1.43-1.32 (2H, m, COD-CH₂).

¹³C NMR (101 MHz, CDCl₃): δ 176.5 (d ²J_{C-P} = 7.7 Hz), 161.2 (q ¹J_{C-B} = 49.5 Hz), 140.4, 135.6, 135.3, 134.3, 134.2, 132.2, 132.1, 130.0, 129.5, 129.33, 129.28, 128.4 (q ²J_{C-F} = 32.9 Hz), 128.3, 127.1, 125.7, 124.1 (q ¹J_{C-F} = 269 Hz), 116.9, 86.1, 85.9, 75.5, 31.3, 31.0, 30.0, 29.7, 20.5, 19.6, 19.0.

³¹P NMR (162 MHz, CDCl₃): δ -7.98 (PBN₃).

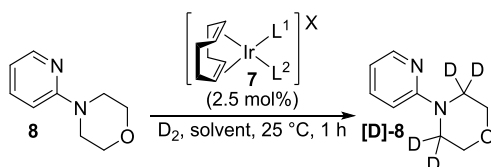
¹⁹F NMR (376 MHz, CDCl₃): δ -62.42 (BARf).

¹¹B NMR (128 MHz, CDCl₃): δ -6.65 (BARf).

HRMS (NSI): m/z calculated for C₅₀H₅₇IrN₂P [M]⁺: 607.3867; found: 607.3860.

See page S29 for spectra.

4. Screening of Catalysts 1a-1g and Extended Solvent Screen (Manuscript Table 1)



Reactions were carried out following the general procedure on page S7, using 4-(pyridin-2-yl)morpholine **2** (14.1 mg, 0.086 mmol, 1 eq), with catalyst (0.00215 mmol, 2.5 mol%) in 1 mL of solvent (0.086 M) under D₂ for 1 h at 25 °C. The full details are tabulated below in **Table S2**. Entries 11-15 are supplementary to the manuscript Table 1 entries.

Each reaction was performed in duplicate. The deuterium incorporation was analysed by LCMS and the deuterium distribution was confirmed by ¹H NMR spectroscopy.

Table S2. Screening of Catalysts **1a-1g** and Extended Solvent Screen.

Entry	Complex	mass (mg) of catalyst used	Solvent	Deuterium Incorporation (%D)		
				Run 1	Run 2	Average
1	 1a	2.2	DCM	76	81	79
2	 1b	3.7	DCM	88	92	90
3	 1c	3.8	DCM	85	84	85
4	 1d	3.5	DCM	75	81	78
5	 1e	1.4	DCM	0	0	0
6	 1f	1.7	DCM	26	22	24
7	 1g	3.3	DCM	25	26	26
8	 1b	3.7	<i>t</i> -AmylOH	76	75	76
9	 1b	3.7	MTBE	87	86	87
10	 1b	3.7	<i>t</i> -BuOAc	86	86	86
11	 1b	3.7	MeOH	65	67	66
12	 1b	3.7	<i>i</i> -PrOH	60	55	58
13	 1b	3.7	2-MeTHF	64	73	69
14	 1b	7.4	CPME	83	83	83
15	 1b	3.7	<i>i</i> -PrOAc	80	72	76

5. Design of Experiment

5.1. Optimisation for Conditions A.

Experimental design was used to assess the effect of varying catalyst loading, reaction time, and reaction concentration [Conditions: **2** (14.1 mg, 0.086 mmol), **1b** (*catalyst loading*), DCM (*concentration*), D₂, 25 °C, (*reaction time*)]. As such, 'high' and 'low' values for each of these three variables were chosen. To generate a series of experiments to study optimal conditions within the variable ranges chosen, Design Expert™ software v9.0 (Stat_Ease Inc., Minneapolis, Mn) was used. This generated a 2 level, 3 factorial design containing three centre points, giving 11 experiments in total. The deuterium incorporation of 4-(pyridin-2-yl)morpholine **2** was used as the response (Table S3).

Table S3. Design of Experiment: Optimisation for Protocol 1

Run ^a	Variable A: Catalyst Loading (mol%)	Amount of 1b (mg (mmol))	Variable B: Reaction Time (min)	Variable C: DCM Volume (mL)	Response: Incorporation (%D)
1 (++-)	1.5	2.2 (0.00129)	40	0.5	52
2 (--+)	0.5	0.7 (0.0043)	20	2.5	24
3 (+++)	1.5	2.2 (0.00129)	40	2.5	94
4 (000)	1.0	1.5 (0.00086)	30	1.5	72
5 (-+-)	0.5	0.7 (0.0043)	40	0.5	45
6 (000)	1.0	1.5 (0.00086)	30	1.5	73
7 (---)	0.5	0.7 (0.0043)	20	0.5	30
8 (+--)	1.5	2.2 (0.00129)	20	0.5	51
9 (000)	1.0	1.5 (0.00086)	30	1.5	69
10 (-++)	0.5	0.7 (0.0043)	40	2.5	37
11 (+-+)	1.5	2.2 (0.00129)	20	2.5	70

^a (+) = high value, (-) low value, and (0) = centre point of a variable. (-+-) = combination of low A, high B, and low C

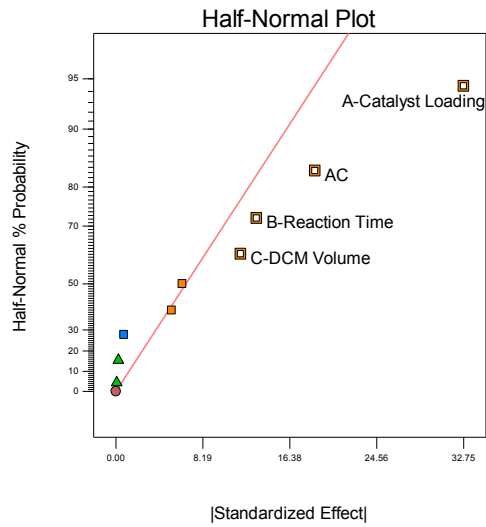
Entries 4, 6, and 9 represent the centre points of the design. These were employed in order to:

- assess any curvature in the response of conversion changes in the variables; and
- assess the repeatability of the hydrogen isotope exchange reaction.

A response surface was created in the same design program. This generated a half-normal plot (**Graph S1**), inferring that increasing the catalyst loading, reaction time, DCM volume, and the combination of catalyst loading and DCM volume have a positive impact upon the efficacy of the labeling reaction.

Design-Expert® Software
Incorporation

- ▲ Error estimates
- A: Catalyst Loading
- B: Reaction Time
- C: DCM Volume
- Positive Effects
- Negative Effects

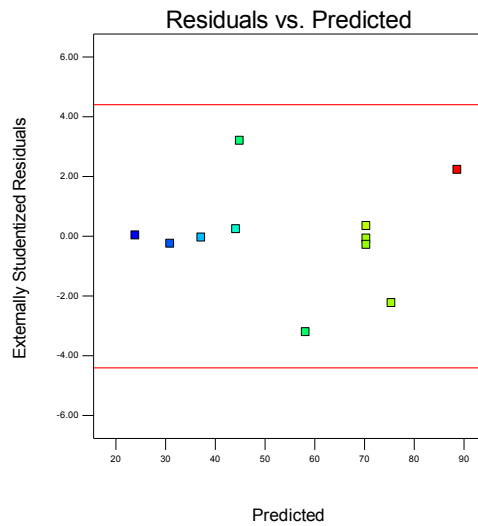


Graph S1

Finally, provided below is a graph of Residuals versus Predicted plot. This is a plot of the residuals versus the ascending predicted response values (lower conversion to higher conversion) and tests the assumption of constant variance in the data (**Graph S2**).

Design-Expert® Software
Incorporation
(adjusted for curvature)

- Color points by value of Incorporation:
- 94
 - 24



Graph S2

5.2. Optimisation for Conditions B

Experimental design was used to assess the effect of varying catalyst loading, reaction time, and reaction concentration [Conditions: **16** (14.0 mg, 0.086 mmol), **1b** (*catalyst loading*), DCM (*concentration*), D₂, 25 °C, (*reaction time*)]. As such, 'high' and 'low' values for each of these three variables were chosen. To generate a series of experiments to study optimal conditions within the variable ranges chosen, Design Expert™ software v9.0 (Stat_Ease Inc., Minneapolis, Mn) was used. This generated a 2 level, 3 factorial design containing three centre points, giving 11 experiments in total. The deuterium incorporation of 4-(pyridin-2-yl)piperazine **16** was used as the response (**Table S4**).

Table S4. Design of Experiment: Optimisation for Protocol 2

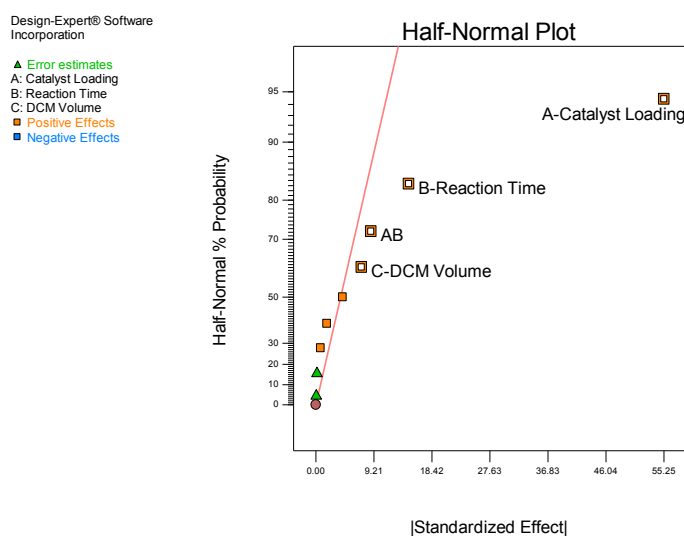
Run ^a	Variable A: Catalyst Loading (mol%)	Amount of 1b (mg (mmol))	Variable B: Reaction Time (min)	Variable C: DCM Volume (mL)	Response: Incorporation (%D)
1 (000)	3.0	4.5	75	1.5	62
2 (+++)	5.0	7.4	120	2.5	83
3 (+--)	5.0	7.4	30	0.5	48
4 (--+)	1.0	1.5	30	2.5	7
5 (000)	3.0	4.5	75	1.5	62
6 (+-+)	5.0	7.4	120	0.5	69
7 (---)	1.0	1.5	30	0.5	5
8 (-+-)	1.0	1.5	120	0.5	10
9 (-++)	1.0	1.5	120	2.5	14
10 (+++)	5.0	7.4	30	2.5	57
11 (000)	3.0	4.5	75	1.5	64

^a (+) = high value, (-) low value, and (0) = centre point of a variable. (-+-) = combination of low A, high B, and low C

Entries 1, 5, and 11 represent the centre points of the design. These were employed in order to:

- assess any curvature in the response of conversion changes in the variables; and
- assess the repeatability of the hydrogen isotope exchange reaction.

A response surface was created in the same design program. This generated a half-normal plot (**Graph S3**), inferring that increasing the catalyst loading, reaction time, DCM volume, and the combination of catalyst loading and DCM volume have a positive impact upon the efficacy of the labelling reaction.



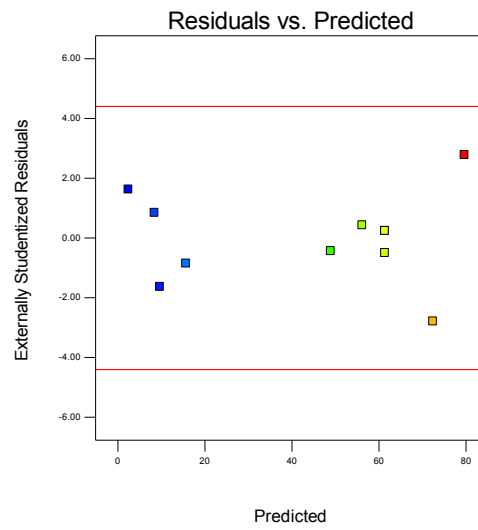
Graph S3

Finally, provided below is a graph of Residuals versus Predicted plot. This is a plot of the residuals versus the ascending predicted response values (lower conversion to higher conversion) and tests the assumption of constant variance in the data (**Graph S4**).

Design-Expert® Software
Incorporation
(adjusted for curvature)

Color points by value of
Incorporation:

83
5



Graph S4

6. Substrate Scope (Manuscript Scheme 2)



Conditions A

Reactions were carried out following the general procedure on page S7, using substrate (0.086 mmol, 1 eq), with catalyst **1b** (1.5 mg, 0.00086 mmol, 1.0 mol%) in 1 mL of DCM (0.086 M) under D₂ for 1 h at 25 °C.

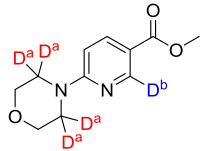
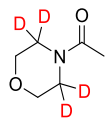
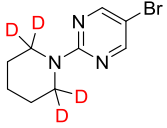

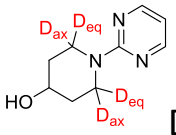
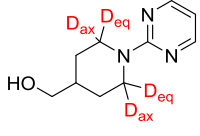
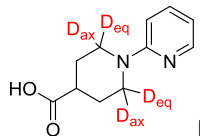
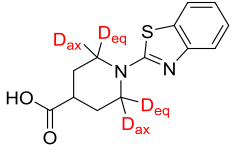
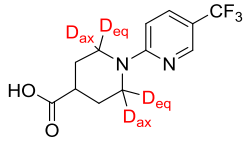
Conditions B

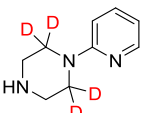
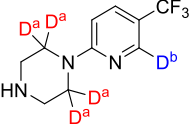
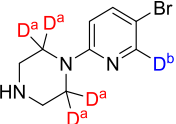
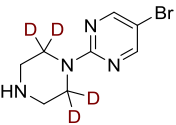
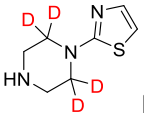
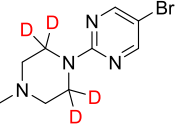
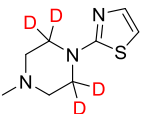
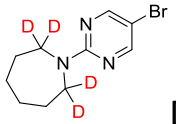
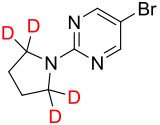
Reactions were carried out following the general procedure on page S7, using substrate (0.086 mmol, 1 eq), with catalyst **1b** (7.4 mg, 0.0043 mmol, 5.0 mol%) in 1 mL of DCM (0.086 M) under D₂ for 3 h at 25 °C.


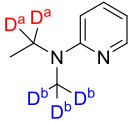
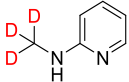
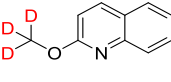
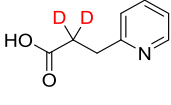
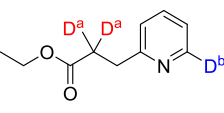
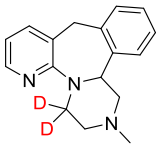
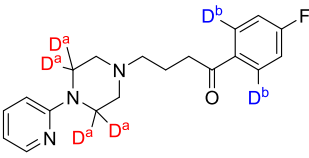
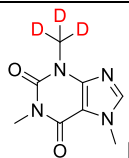
Each reaction was performed in duplicate. The extent and position of labeling was established using ¹H NMR spectroscopy. The average deuterium incorporation for each molecule across all labeled positions was further confirmed by LCMS analysis. The details of the substrate scope described within the manuscript are given in **Table S5** below.

Table S5. Substrate Scope.

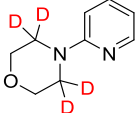
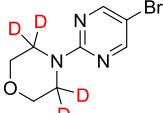
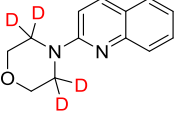
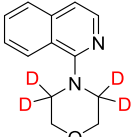
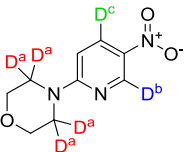
Entry	Substrate	Mass of Substrate Used (mg)	Protocol	Deuterium Incorporation (%D)			¹ H NMR Distribution
				LC-MS			
				Run 1	Run 2	Average	
1	 [D]-2	14.1	A	82	78	80	80
2	 [D]-3	21.0	A	95	95	95	95
3	 [D]-4	18.4	A	85	91	88	94
4	 [D]-5	18.4	A	96	92	94	99
5	 [D]-6	18.0	A	85	86	86	D ^a = 87 D ^b = 91 D ^c = 57

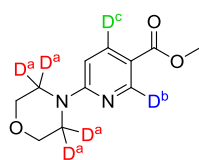
6		19.1	A	82	83	83	$D^a = 95$ $D^b = 5$
7		11.1	A B*	0 11	0 13	0 12	0 12
8		20.8	A	94	96	95	91
9		14.5	A	78	82	80	86
10		15.4	A	88	90	89	$D_{ax} = 83$ $D_{eq} = 84$
11		16.6	A	89	89	89	$D_{ax} = 86$ $D_{eq} = 89$
12		17.7	A	78	83	81	$D_{ax} = 73$ $D_{eq} = 87$
13		22.6	A**	83	81	82	$D_{ax} = 77$ $D_{eq} = 87$
14		23.6	A	95	89	92	$D_{ax} = 90$ $D_{eq} = 93$

15	 [D]-16	14.0	A	17	18	18	18
			B	90	94	92	89
16	 [D]-17	19.9	A	11	12	12	$D^a = 11$
			B	64	70	67	$D^b = 0$
17	 [D]-18	20.8	A	24	25	25	$D^a = 24$
			B	86	86	86	$D^b = 0$
18	 [D]-19	20.9	A	7	8	8	$D^a = 24$
			B	77	82	80	$D^b = 0$
19	 [D]-20	14.6	A	24	19	22	$D^a = 92$
			B	90	90	90	$D^b = 34$
20	 [D]-21	22.1	A	87	94	91	$D^a = 24$
			B	90	90	90	$D^b = 34$
21	 [D]-22	15.8	A	87	82	85	$D^a = 92$
			B	90	90	90	$D^b = 34$
22	 [D]-23	22.0	A	47	47	47	$D^a = 92$
			B	86	84	85	$D^b = 34$
23	 [D]-24	19.6	A	58	56	57	$D^a = 92$
			B	94	94	94	$D^b = 34$

24	 [D]-25	18.4	A	0	0	0	0
			B	8	9	9	9
25	 [D]-26	11.7	A	0	0	0	D ^a = 0
			B	96	95	96	D ^b = 0
26	 [D]-27	9.3	A	0	0	0	0
			B	32	28	30	37
27	 [D]-28	13.7	A	13	15	14	14
			B	70	77	74	80
28	 [D]-29	13.0	A	16	19	18	16
			B	58	63	61	65
29	 [D]-30	15.4	A	0	0	0	D ^a = 0
			B	25	21	23	D ^b = 0
30	 [D]-31	22.8	A	95	94	95	94
			B				
31	 [D]-32	28.2	A	71	72	72	D ^a = 97
			B				D ^b = 13
32	 [D]-33	16.7	A	41	41	41	41
			B	93	91	92	92

* Reaction conditions = substrate (0.086 mmol, 1 eq), with catalyst **1b**, (7.4 mg, 0.0043 mmol, 5.0 mol%) in 1 mL of MTBE (0.086 M) under D₂ for 3 h at 50 °C. ** Reaction conditions = substrate (0.086 mmol, 1 eq), with catalyst **1b**, (1.5 mg, 0.00086 mmol, 1.0 mol%) in 1 mL of 2-MeTHF (0.086 M) under D₂ for 1 h at 25 °C.

Substrate	¹ H NMR data ⁴
 <p data-bbox="347 315 411 340">[D]-2</p>	<p data-bbox="552 136 1509 277">¹H NMR (300 MHz, DMSO-d₆): δ 8.12 (1H, dd, <i>J</i> = 5.1 Hz, ⁴<i>J</i> = 1.5 Hz, Ar-H), 7.54 (1H, ddd, <i>J</i> = 8.7 Hz, 7.1 Hz, ⁴<i>J</i> = 1.5 Hz, Ar-H), 6.81 (1H, d, <i>J</i> = 8.7 Hz, Ar-H), 6.66 (1H, dd, <i>J</i> = 7.7 Hz, ⁴<i>J</i> = 5.1 Hz, Ar-H), 3.72-3.64 (4H, m, O-CH₂), 3.44-3.37 (4H, m, N-CH₂).</p> <p data-bbox="552 282 1015 309">Incorporation expected at δ 3.44-3.37.</p> <p data-bbox="552 315 1007 344">Determined against integral at δ 6.66.</p>
LCMS data	
Retention time: 0.28 min; Mass ion: 165.1 (M+H) ⁺	
¹H NMR data⁵	
 <p data-bbox="360 645 427 669">[D]-3</p>	<p data-bbox="552 533 1437 562">¹H NMR (300 MHz, DMSO-d₆): δ 8.46 (2H, s, Ar-H), 3.70-3.60 (8H, m, CH₂).</p> <p data-bbox="552 568 1015 595">Incorporation expected at δ 3.70-3.60.</p> <p data-bbox="552 602 1007 631">Determined against integral at δ 8.46.</p>
LCMS data	
Retention time: 2.69 min; Mass ion: 244.1 (M+H) ⁺ [using ⁷⁹ Br]	
¹H NMR data⁶	
 <p data-bbox="368 960 432 985">[D]-4</p>	<p data-bbox="552 824 1509 927">¹H NMR (300 MHz, DMSO-d₆): δ 8.05 (1H, d, <i>J</i> = 9.3 Hz, Ar-H), 7.70 (1H, d, <i>J</i> = 7.9 Hz, Ar-H), 7.61-7.48 (2H, m, Ar-H), 7.28-7.18 (2H, m, Ar-H), 3.76-3.69 (4H, m, O-CH₂), 3.68-3.59 (4H, m, N-CH₂).</p> <p data-bbox="552 931 1015 958">Incorporation expected at δ 3.68-3.59.</p> <p data-bbox="552 965 1067 994">Determined against integral at δ 7.28-7.18.</p>
LCMS data	
Retention time: 0.49 min; Mass ion: 215.1 (M+H) ⁺	
¹H NMR data⁷	
 <p data-bbox="347 1339 411 1364">[D]-5</p>	<p data-bbox="552 1182 1509 1285">¹H NMR (300 MHz, DMSO-d₆): δ 8.15-8.08 (2H, m, Ar-H), 7.88 (1H, d, <i>J</i> = 8.2 Hz, Ar-H), 7.75-7.66 (1H, m, Ar-H), 7.63-7.54 (1H, m, Ar-H), 7.39 (1H, d, <i>J</i> = 5.7 Hz, Ar-H), 3.90-3.80 (4H, m, O-CH₂), 3.33-3.27 (4H, m, N-CH₂).</p> <p data-bbox="552 1290 1015 1317">Incorporation expected at δ 3.33-3.27.</p> <p data-bbox="552 1323 1007 1352">Determined against integral at δ 7.39.</p>
LCMS data	
Retention time: 0.80 min; Mass ion: 215.1 (M+H) ⁺	
¹H NMR data⁸	
 <p data-bbox="379 1680 443 1704">[D]-6</p>	<p data-bbox="552 1541 1509 1610">¹H NMR (300 MHz, DMSO-d₆): δ 8.96 (1H, d, ⁴<i>J</i> = 2.8 Hz, Ar-H), 8.23 (1H, dd, <i>J</i> = 9.6 Hz, ⁴<i>J</i> = 2.8 Hz, Ar-H), 6.93 (1H, d, <i>J</i> = 9.6 Hz, Ar-H), 3.81-3.59 (8H, m, CH₂).</p> <p data-bbox="552 1615 1259 1641">Incorporation expected at δ D^a 3.81-3.59, D^b 8.96, D^c 8.23.</p> <p data-bbox="552 1648 1015 1677">Determined against integral at δ 6.93.</p>
LCMS data	
Retention time: 2.38 min; Mass ion: 210.1 (M+H) ⁺	



[D]-7

¹H NMR data⁹

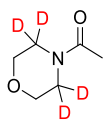
¹H NMR (300 MHz, DMSO-d₆): δ 8.65 (1H, d, ⁴J = 2.5 Hz, Ar-H), 7.96 (1H, dd, J = 9.1 Hz, ⁴J = 2.4 Hz, Ar-H), 6.87 (1H, d, J = 9.2 Hz, Ar-H), 3.78 (3H, s, O-CH₃), 3.71-3.64 (4H, m, O-CH₂), 3.63-3.56 (4H, m, N-CH₂).

Incorporation expected at δ D^a 3.63-3.56, D^b 8.65, D^c 7.96.

Determined against integral at δ 3.78.

LCMS data

Retention time: 2.00 min; Mass ion: 223.2 (M+H)⁺



[D]-8

¹H NMR data¹⁰

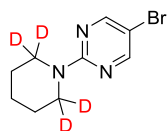
¹H NMR (300 MHz, DMSO-d₆): δ 3.59-3.48 (4H, m, O-CH₂), 3.45-3.36 (4H, m, N-CH₂), 1.97 (3H, s, CO-CH₃).

Incorporation expected at δ 3.45-3.36.

Determined against integral at δ 1.97.

LCMS data

Retention time: 0.41 min; Mass ion: 130.1 (M+H)⁺



[D]-9

¹H NMR data¹¹

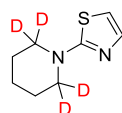
¹H NMR (300 MHz, DMSO-d₆): δ 8.38 (2H, br s, Ar-H), 3.75-3.62 (4H, m, N-CH₂), 1.66-1.56 (2H, m, CH₂), 1.55-1.43 (4H, m, CH₂).

Incorporation expected at δ 3.75-3.62.

Determined against integral at δ 1.55-1.43.

LCMS data

Retention time: 3.54 min; Mass ion: 242.1 (M+H)⁺ [using ⁷⁹Br]



[D]-10

¹H NMR data¹²

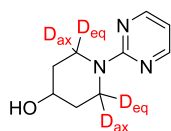
¹H NMR (300 MHz, DMSO-d₆): δ 7.11 (1H, d, J = 3.7 Hz, Ar-H), 6.75 (1H, d, J = 3.6 Hz, Ar-H), 3.45-3.33 (4H, m, N-CH₂), 1.65-1.52 (6H, m, CH₂).

Incorporation expected at δ 3.45-3.33.

Determined against integral at δ 1.65-1.52.

LCMS data

Retention time: 0.67 min; Mass ion: 169.0 (M+H)⁺



[D]-11

¹H NMR data¹³

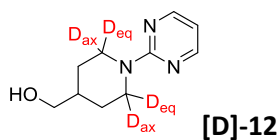
¹H NMR (300 MHz, DMSO-d₆): δ 8.31 (2H, d, J = 4.7 Hz, Ar-H), 6.55 (1H, t, J = 4.7 Hz, Ar-H), 4.64 (1H, d, J = 4.2 Hz, O-H), 4.24 (2H, ddd, ²J = 13.0 Hz, J = 5.6 Hz, 4.1 Hz, N-CH₂), 3.72 (1H, oct, J = 4.2 Hz, O-CH), 3.24 (2H, ddd, ²J = 13.0 Hz, J = 9.1 Hz, 3.7 Hz, N-CH₂), 1.81-1.70 (2H, m, CH₂), 1.39-1.23 (2H, m, CH₂).

Incorporation expected at δ 3.24 axial, 4.24 equatorial.

Determined against integral at δ 1.39-1.23.

LCMS data

Retention time: 0.72 min; Mass ion: 180.1 (M+H)⁺



¹H NMR data¹⁴

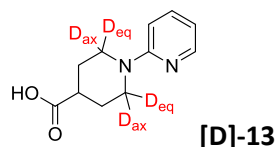
¹H NMR (300 MHz, DMSO-d₆): δ 8.30 (2H, d, *J* = 4.7 Hz, Ar-H), 6.53 (1H, t, *J* = 4.7 Hz, Ar-H), 4.70-4.58 (2H, m, N-CH₂), 4.40 (1H, t, *J* = 5.3 Hz, O-H), 3.33-3.20 (2H, m, O-CH₂), 2.83 (2H, td, *J* = 12.7 Hz, 2.7 Hz, N-CH₂), 1.77-1.55 (3H, m, CH₂-CH & CH₂), 1.14-0.95 (2H, m, CH₂).

Incorporation expected at δ 2.83 axial, 4.70-4.58 equatorial.

Determined against integral at δ 1.14-0.95.

LCMS data

Retention time: 0.71 min; Mass ion: 194.1 (M+H)⁺



¹H NMR data¹⁵

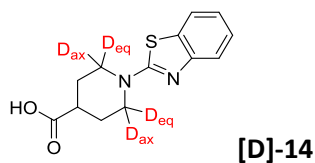
¹H NMR (300 MHz, DMSO-d₆): δ 12.15 (1H, br s, O-H), 8.08 (1H, dd, *J* = 5.2 Hz, ⁴*J* = 2.0 Hz, Ar-H), 7.49 (1H, ddd, *J* = 8.7 Hz, 7.1 Hz, ⁴*J* = 2.0 Hz, Ar-H), 6.80 (1H, d, *J* = 8.7 Hz, Ar-H), 6.58 (1H, dd, *J* = 7.1 Hz, 5.2 Hz, Ar-H), 4.16 (2H, ddd, ²*J* = 13.3 Hz, *J* = 4.3 Hz, 3.2 Hz, N-CH₂), 2.92 (2H, ddd, ²*J* = 13.3 Hz, *J* = 11.5 Hz, 2.9 Hz, N-CH₂), 2.52-2.42 (1H, m, CH), 1.91-1.79 (2H, m, CH₂), 1.61-1.40 (2H, m, CH₂).

Incorporation expected at δ 2.92 axial, 4.16 equatorial.

Determined against integral at δ 1.61-1.40.

LCMS data

Retention time: 0.39 min; Mass ion: 207.1 (M+H)⁺



¹H NMR data¹⁶

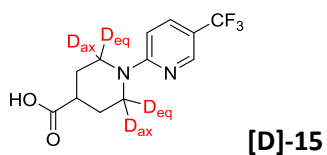
¹H NMR (300 MHz, CD₃CN): δ 9.05 (1H, br-s, O-H), 7.68 (1H, d, *J* = 7.5 Hz, ⁴*J* = 1.5 Hz, Ar-H), 7.44 (1H, d, *J* = 7.5 Hz, Ar-H), 7.28 (1H, td, *J* = 7.5 Hz, ⁴*J* = 1.5 Hz, Ar-H), 7.07 (1H, td, *J* = 7.5 Hz, ⁴*J* = 1.5 Hz, Ar-H), 4.04 (2H, ddd, ²*J* = 12.6 Hz, *J* = 4.2 Hz, 4.1 Hz, N-CH₂), 3.25 (2H, ddd, ²*J* = 12.6 Hz, *J* = 11.4 Hz, 3.0 Hz, N-CH₂), 2.62 (1H, tt, *J* = 11.1 Hz, 4.0 Hz, CH), 2.07-1.96 (2H, m, CH₂), 1.81-1.64 (2H, m, CH₂).

Incorporation expected at δ axial 3.25, equatorial 4.04.

Determined against integral at δ 1.81-1.64.

LCMS data

Retention time: 2.49 min; Mass ion: 263.1 (M+H)⁺



¹H NMR data¹⁷

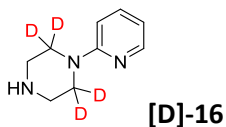
¹H NMR (300 MHz, DMSO-d₆): δ 12.11 (1H, br s, O-H), 8.37 (1H, br s, Ar-H), 7.74 (1H, dd, *J* = 9.1 Hz, ⁴*J* = 2.6 Hz, Ar-H), 6.93 (1H, d, *J* = 9.1 Hz, Ar-H), 4.27 (2H, ddd, ²*J* = 13.5 Hz, *J* = 3.8 Hz, 3.8 Hz, N-CH₂), 3.08 (2H, ddd, ²*J* = 13.5 Hz, *J* = 11.2 Hz, 3.0 Hz, N-CH₂), 2.56 (1H, tt, *J* = 11.0 Hz, 4.0 Hz, CH), 1.94-1.81 (2H, m, CH₂), 1.61-1.41 (2H, m, CH₂).

Incorporation expected at δ 3.08 axial, 4.27 equatorial.

Determined against integral at δ 1.61-1.41.

LCMS data

Retention time: 3.19 min; Mass ion: 275.1 (M+H)⁺



¹H NMR data¹⁸

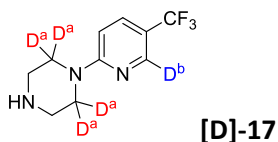
¹H NMR (300 MHz, DMSO-d₆): δ 8.08 (1H, dd, *J* = 4.9 Hz, ⁴*J* = 2.1 Hz, Ar-H), 7.49 (1H, ddd, *J* = 8.7 Hz, 7.1 Hz, ⁴*J* = 2.1 Hz, Ar-H), 6.75 (1H, d, *J* = 8.7 Hz, Ar-H), 6.59 (1H, dd, *J* = 7.1 Hz, 4.9 Hz, Ar-H), 3.43-3.32 (4H, m, N-CH₂), 2.81-2.70 (4H, m, NH-CH₂).

Incorporation expected at δ 3.43-3.32.

Determined against integral at δ 2.81-2.70.

LCMS data

Retention time: 0.37 min; Mass ion: 164.0 (M+H)⁺



¹H NMR data¹⁹

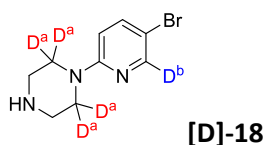
¹H NMR (300 MHz, DMSO-d₆): δ 8.37 (1H, br s, Ar-H), 7.73 (1H, dd, *J* = 9.1 Hz, ⁴*J* = 2.7 Hz, Ar-H), 6.88 (1H, d, *J* = 9.1 Hz, Ar-H), 3.59-3.48 (4H, m, N-CH₂), 2.88-2.60 (4H, m, NH-CH₂).

Incorporation expected at δ D^a 3.59-3.48, D^b 8.37.

Determined against integral at δ 2.88-2.60.

LCMS data

Retention time: 1.12 min; Mass ion: 232.3 (M+H)⁺



¹H NMR data²⁰

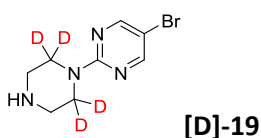
¹H NMR (300 MHz, DMSO-d₆): δ 8.40 (1H, br s, Ar-H), 7.77 (1H, dd, *J* = 9.2 Hz, ⁴*J* = 2.5 Hz, Ar-H), 6.92 (1H, d, *J* = 9.4 Hz, Ar-H), 3.64-3.46 (4H, m, N-CH₂), 2.88-2.71 (4H, m, NH-CH₂).

Incorporation expected at δ D^a 3.64-3.46, D^b 8.40.

Determined against integral at δ 2.88-2.71.

LCMS data

Retention time: 2.24 min; Mass ion: 242.1 (M+H)⁺ [using ⁷⁹Br]



¹H NMR data²¹

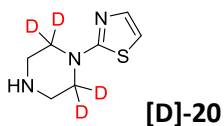
¹H NMR (300 MHz, DMSO-d₆): 8.46 (2H, br s, Ar-H), 3.89-3.75 (4H, m, N-CH₂), 2.90-2.78 (4H, m, NH-CH₂).

Incorporation expected at δ 3.89-3.75.

Determined against integral at δ 2.90-2.78.

LCMS data

Retention time: 2.24 min; Mass ion: 243.1 (M+H)⁺ [using ⁷⁹Br]



¹H NMR data²²

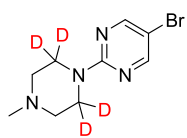
¹H NMR (300 MHz, DMSO-d₆): δ 7.14 (1H, d, *J* = 3.6 Hz, Ar-H), 6.79 (1H, d, *J* = 3.6 Hz, Ar-H), 3.36-3.26 (4H, m, N-CH₂), 2.83-2.73 (4H, m, NH-CH₂).

Incorporation expected at δ 3.36-3.26.

Determined against integral at δ 2.83-2.73.

LCMS data

Retention time: 0.29 min; Mass ion: 170.1 (M+H)⁺



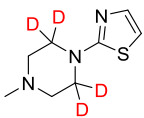
[D]-21

¹H NMR data²³

¹H NMR (300 MHz, DMSO-d₆): δ 8.42 (2H, s, Ar-H), 3.76-3.63 (4H, m, N-CH₂), 2.38-2.29 (4H, m, NMe-CH₂), 2.19 (3H, s, N-CH₃).
Incorporation expected at δ 3.76-3.63.
Determined against integral at δ 2.19.

LCMS data

Retention time: 0.41 min; Mass ion: 257.1 (M+H)⁺ [using ⁷⁹Br]



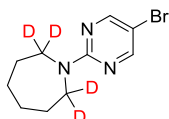
[D]-22

¹H NMR data²⁴

¹H NMR (300 MHz, DMSO-d₆): δ 7.15 (1H, d, *J* = 3.6 Hz, Ar-H), 6.81 (1H, d, *J* = 3.6 Hz, Ar-H), 3.43-3.33 (4H, m, N-CH₂), 2.46-2.35 (4H, m, NMe-CH₂), 2.21 (3H, s, N-CH₃).
Incorporation expected at δ 3.43-3.33.
Determined against integral at δ 2.21.

LCMS data

Retention time: 0.29 min; Mass ion: 184.1 (M+H)⁺



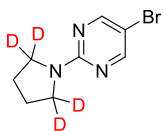
[D]-23

¹H NMR data²⁵

¹H NMR (300 MHz, DMSO-d₆): δ 8.39 (2H, br s, Ar-H), 3.73-3.60 (4H, m, N-CH₂), 1.77-1.61 (4H, m, CH₂), 1.54-1.39 (4H, m, CH₂).
Incorporation expected at δ 3.73-3.60.
Determined against integral at δ 1.54-1.39.

LCMS data

Retention time: 0.29 min; Mass ion: 256.1 (M+H)⁺ [using ⁷⁹Br]



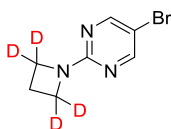
[D]-24

¹H NMR data²⁶

¹H NMR (300 MHz, DMSO-d₆): δ 8.40 (2H, br s, Ar-H), 3.53-3.38 (4H, m, N-CH₂), 2.01-1.85 (4H, m, CH₂).
Incorporation expected at δ 3.53-3.38.
Determined against integral at δ 2.01-1.85.

LCMS data

Retention time: 2.85 min; Mass ion: 228.1 (M+H)⁺ [using ⁷⁹Br]



[D]-25

¹H NMR data²⁷

¹H NMR (300 MHz, DMSO-d₆): δ 8.40 (2H, br s, Ar-H), 4.02 (4H, t, *J* = 7.5 Hz, N-CH₂), 2.30 (2H, quin, *J* = 7.6 Hz, CH₂).
Incorporation expected at δ D 4.02.
Determined against integral at δ 2.30.

LCMS data

Retention time: 2.30 min; Mass ion: 214.0 (M+H)⁺ [using ⁷⁹Br]



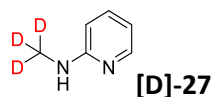
[D]-26

¹H NMR data²⁸

¹H NMR (300 MHz, DMSO-d₆): δ 8.04 (1H, dd, *J* = 4.9 Hz, ⁴*J* = 2.1 Hz, Ar-H), 7.45 (1H, ddd, *J* = 8.7 Hz, 7.1 Hz, ⁴*J* = 2.1 Hz, Ar-H), 6.57 (1H, d, *J* = 8.7 Hz, Ar-H), 6.50 (1H, dd, *J* = 7.1 Hz, 4.8 Hz, Ar-H), 3.53 (2H, q, *J* = 7.1 Hz, N-CH₂), 2.94 (3H, s, N-CH₃), 1.05 (3H, t, *J* = 7.1 Hz, CH₂-CH₃).
Incorporation expected at δ D^a 3.53, D^b 2.94.
Determined against integral at δ 1.05.

LCMS data

Retention time: 0.30 min; Mass ion: 137.2 (M+H)⁺



¹H NMR data²⁹

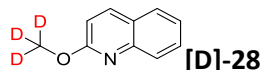
¹H NMR (300 MHz, DMSO-d₆): δ 7.96 (1H, dd, *J* = 5.0 Hz, ⁴*J* = 2.0 Hz, Ar-H), 7.34 (1H, ddd, *J* = 8.4 Hz, 7.0 Hz, ⁴*J* = 2.0 Hz, Ar-H), 6.50-6.37 (2H, m, Ar-H), 6.31 (1H, br s, N-H), 2.75 (3H, d, *J* = 4.9 Hz, NH-CH₃).

Incorporation expected at δ 2.75.

Determined against integral at δ 7.34.

LCMS data

Retention time: 0.25 min; Mass ion: 109.2 (M+H)⁺



¹H NMR data³⁰

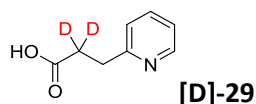
¹H NMR (300 MHz, DMSO-d₆): δ 8.21 (1H, d, *J* = 8.9 Hz, Ar-H), 7.86 (1H, dd, *J* = 7.8 Hz, ⁴*J* = 1.6 Hz, Ar-H), 7.78 (1H, d, *J* = 8.3 Hz, Ar-H), 7.65 (1H, ddd, *J* = 8.4 Hz, 7.0 Hz, ⁴*J* = 1.6 Hz, Ar-H), 7.42 (1H, ddd, *J* = 8.1 Hz, 6.9 Hz, ⁴*J* = 1.4 Hz, Ar-H), 7.00 (1H, d, *J* = 8.9 Hz, Ar-H), 3.98 (3H, s, O-CH₃).

Incorporation expected at δ 3.98.

Determined against integral at δ 7.00.

LCMS data

Retention time: 3.00 min; Mass ion: 160.1 (M+H)⁺



¹H NMR data³¹

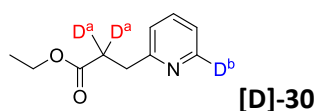
¹H NMR (300 MHz, DMSO-d₆): δ 12.10 (1H, br s, O-H), 8.46 (1H, dd, *J* = 5.1 Hz, ⁴*J* = 1.9 Hz, Ar-H), 7.68 (1H, dd, *J* = 7.7 Hz, ⁴*J* = 1.9 Hz, Ar-H), 7.26 (1H, d, *J* = 7.9 Hz, Ar-H), 7.19 (1H, dd, *J* = 7.7 Hz, 5.0 Hz, Ar-H), 2.96 (2H, t, *J* = 7.4 Hz, Ar-CH₂), 2.65 (2H, t, *J* = 7.4 Hz, CO-CH₂).

Incorporation expected at δ 2.65.

Determined against integral at δ 7.68.

LCMS data

Retention time: 0.29 min; Mass ion: 152.1 (M+H)⁺



¹H NMR data³²

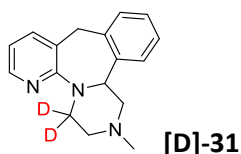
¹H NMR (300 MHz, DMSO-d₆): δ 8.45 (1H, d, *J* = 4.9 Hz, Ar-H), 7.68 (1H, td, *J* = 7.7 Hz, ⁴*J* = 1.8 Hz, Ar-H), 7.26 (1H, d, *J* = 7.5 Hz, Ar-H), 7.18 (1H, dd, *J* = 7.3 Hz, 4.8 Hz, Ar-H), 4.02 (2H, q, *J* = 7.2 Hz, O-CH₂), 2.99 (2H, t, *J* = 7.3 Hz, Ar-CH₂), 2.72 (2H, t, *J* = 7.3 Hz, CO-CH₂), 1.13 (3H, t, *J* = 7.2 Hz, CH₂-CH₃).

Incorporation expected at δ D^a: 2.72, D^b: 8.45.

Determined against integral at δ 1.13.

LCMS data

Retention time: 0.46 min; Mass ion: 180.2 (M+H)⁺



¹H NMR data³³

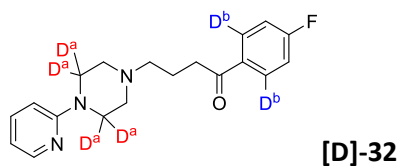
¹H NMR (300 MHz, DMSO-d₆): δ 8.08 (1H, dd, *J* = 4.9 Hz, ⁴*J* = 1.9 Hz, Ar-H), 7.43 (1H, d, *J* = 7.3 Hz, Ar-H), 7.30-7.07 (4H, m, Ar-H), 6.77 (1H, dd, *J* = 7.3 Hz, 4.9 Hz, Ar-H), 4.39-4.19 (2H, m, N-CH & Ar-CH₂), 3.67 (1H, d, ²*J* = 13.5 Hz, Ar-CH₂), 3.48-3.36 (2H, m, N-CH₂), 2.84-2.66 (2H, m, NMe-CH₂), 2.52-2.45 (1H, m, NMe-CH₂), 2.36-2.19 (4H, m, N-CH₃ & NMe-CH₂).

Incorporation expected at δ 3.48-3.36.

Determined against integral at δ 3.67.

LCMS data

Retention time: 0.50 min; Mass ion: 266.3 (M+H)⁺



¹H NMR data³⁴

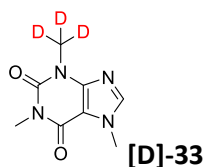
¹H NMR (300 MHz, DMSO-d₆): δ 8.15-7.91 (3H, m, Ar-H), 7.49 (1H, ddd, *J* = 8.5 Hz, 7.7 Hz, ⁴*J* = 2.2 Hz, Ar-H), 7.39-7.24 (2H, m, Ar-H), 6.76 (1H, d, *J* = 8.6 Hz, Ar-H), 6.60 (1H, dd, *J* = 7.7 Hz, 4.8 Hz, Ar-H), 3.43-3.32 (4H, m, Ar-N-CH₂), 3.01 (2H, t, *J* = 7.0 Hz, N-CH₂), 2.45-2.27 (6H, m, CH₂ & N-CH₂), 1.90-1.77 (2H, m, CH₂).

Incorporation expected at δ D^a 3.43-3.32, D^b 8.15-7.91.

Determined against integral at δ 1.90-1.77.

LCMS data

Retention time: 0.38 min; Mass ion: 328.4 (M+H)⁺



¹H NMR data³⁵

¹H NMR (300 MHz, DMSO-d₆): δ 7.98 (1H, s, Ar-H), 3.87 (3H, s, N-CH₃), 3.40 (3H, s, N-CH₃), 3.21 (3H, s, N-CH₃).

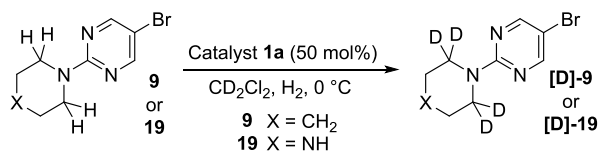
Incorporation expected at δ 3.40.

Determined against integral at δ 3.87.

LCMS data

Retention time: 0.92 min; Mass ion: 195.1 (M+H)⁺

7. NMR Studies Regarding Piperazine NH Binding



Experiments were run to determine the effect of secondary amines on the unactivated pre-catalyst, and activated catalyst species. Below, “Unactivated” refers to experiments run without catalyst activation with H₂, and “Activated” refers to experiments run after catalyst activation with H₂.

“Activated” protocol: In an oven dried NMR tube, substrate (**9**: 4.8 mg, 0.02 mmol or **19**: 4.9 mg, 0.02 mmol), catalyst **1a** (10 mg, 0.01 mmol) and DCM (0.5 mL) were added and the tube capped with a rubber septum. Hydrogen was bubbled through the solution at a constant rate for 5 min to activate the catalyst, and a red to yellow colour change was observed. Following the catalyst activation the NMR tube was cooled to 0 °C in an ice bath prior to injection into the NMR spectrometer. ³¹P NMR experiments were run at 0 °C to allow observation of changes in the active catalytic species.

“Unactivated” protocol: This follows the above “Activated” protocol, but without the introduction of hydrogen gas.

³¹P NMR data for the experiments are displayed below (Fig. S2).

The experiments reveal that when unactivated, the pre-catalyst remains unaffected by the substrate, showing the same shift of 18.3 ppm. Similarly, in the case of piperidine-containing substrate **9** a single catalytic species is formed, with a ³¹P NMR shift of 24.9 ppm after activation. However, with piperazine containing substrate **19**, several signals are observed, with none appearing at 24.9 ppm, clearly indicating several different phosphine-containing species are being formed.

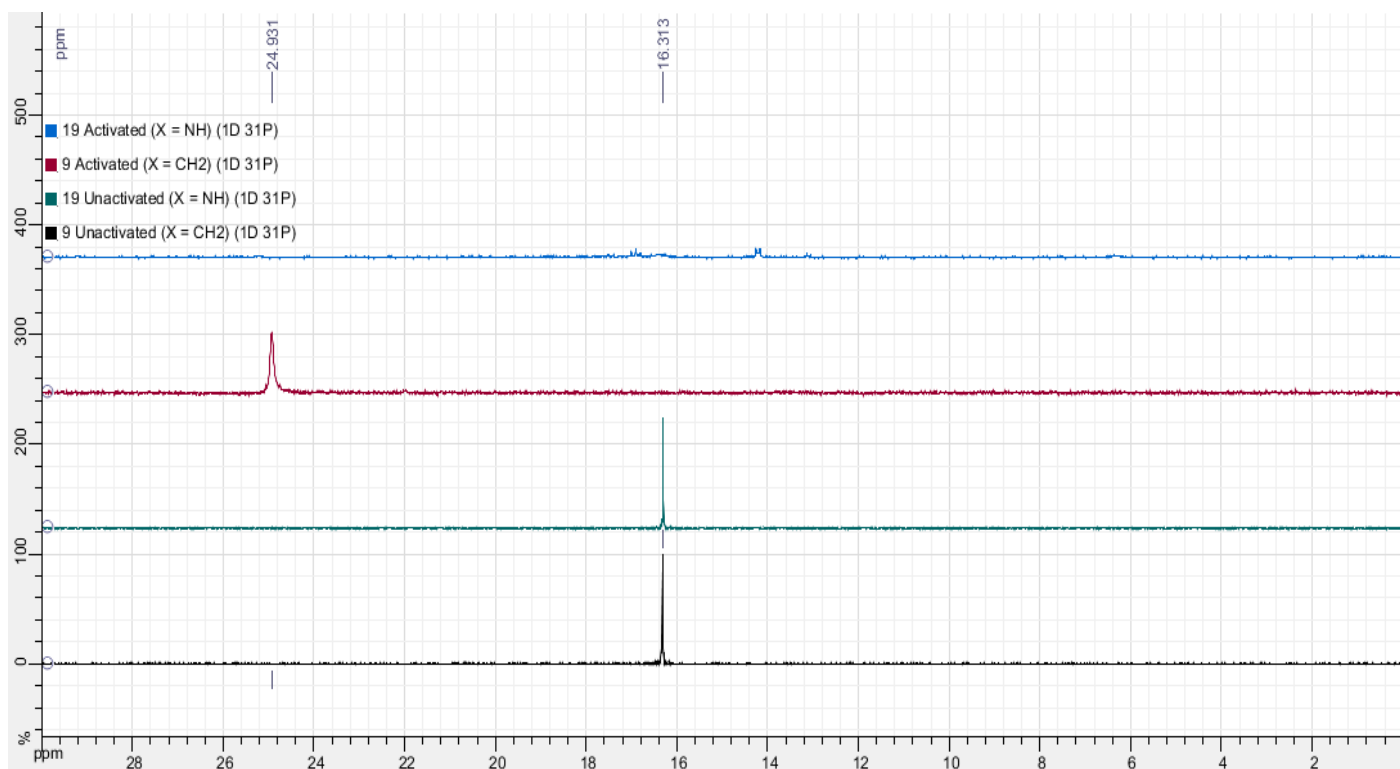
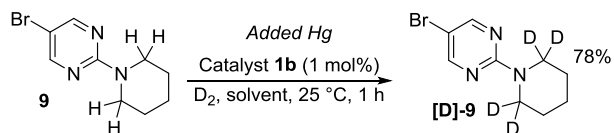


Figure S2.

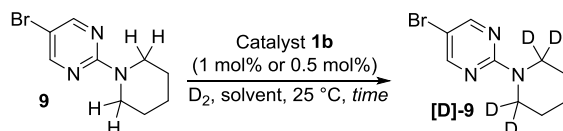
8. Mechanistic Investigations

8.1. Mercury Nanoparticle Test



The reaction was carried out as described on page S7, except with the addition of a mercury drop prior to catalyst activation with D_2 . The reaction proceeded to similarly high incorporation (78%) as without added mercury (91%), indicating that the reaction is homogeneous in nature, and is not catalysed by heterogeneous nanoparticles formed *in situ*.

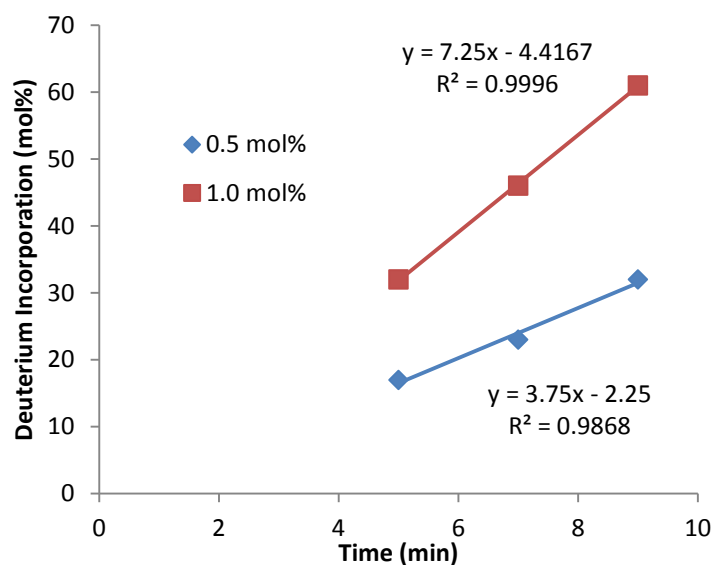
8.2. Order of Reaction



Reactions were carried out following the general procedure on page S7, using 5-bromo-2-(piperidin-1-yl)pyrimidine **9** (20.8 mg, 0.086 mmol, 1 eq), with catalyst **1b** (1.5 mg, 0.00086 mmol, 1.0 mol% or 0.7 mg, 0.00043 mmol, 0.5 mol%) in 1 mL of solvent (0.086 M) under an atmosphere of D_2 for the stated time at 25 °C. The deuterium incorporation was assigned by 1H NMR spectroscopy. The full incorporation data are given below in **Table S6**, and in **Graph S5**.

Table S6. Reactions carried out to determine the order of the reaction with respect to catalyst.

Entry	Time (min)	Catalyst Loading (mol%)	Deuterium Incorporation (%D)
1	3	0.5	8
2	3	1.0	12
3	5	0.5	17
4	5	1.0	32
5	7	0.5	23
6	7	1.0	46
7	9	0.5	32
8	9	1.0	61
9	11	0.5	39
10	11	1.0	67

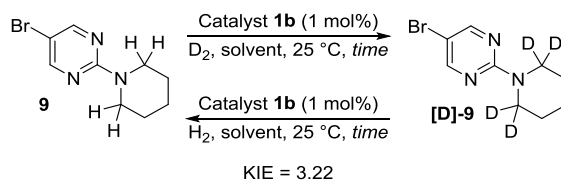


Graph S5. Rate study to determine the order of reaction with respect to catalyst.

The data points for 3 min were discarded as they could occur within the catalyst activation period. The data points for 11 min were discarded as product inhibition has been observed when the incorporation is >60%.

The gradient of the line is proportional to the reaction rate constant. Therefore, the rate increases by a factor of 1.93 ($1.93 \approx 2$) in changing the catalyst loading from 0.5 to 1.0, indicating a first order rate dependence upon the catalyst.

8.3. Kinetic Isotope Effect



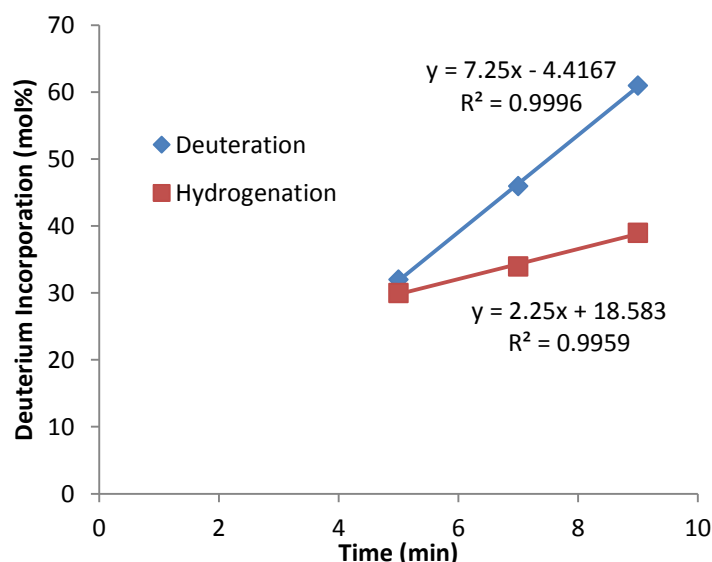
Reactions to incorporate deuterium were carried out following the general procedure on page S7, using 5-bromo-2-(piperidin-1-yl)pyrimidine **9** (20.8 mg, 0.086 mmol, 1 eq), with catalyst (0.00086 mmol, 1.0 mol%) in 1 mL of solvent (0.086 M) under an atmosphere of D₂ for the stated time at 25 °C.

Reactions to incorporate hydrogen were carried out following the general procedure on page S7, using 5-bromo-2-(2,2',6,6'-d₄-piperidin-1-yl)pyrimidine [**D**]-**9** (21.1 mg, 0.086 mmol, 1 eq), with catalyst (0.00086 mmol, 1.0 mol%) in 1 mL of solvent (0.086 M) under an atmosphere of H₂ for the stated time at 25 °C.

The deuterium/hydrogen incorporation was assigned by ¹H NMR spectroscopy. The full incorporation data are given below in **Table S7**, and **Graph S6**.

Table S7. Reactions carried out to determine the kinetic isotope effect.

Entry	Time (min)	Substrate used	Isotope Introduced	Incorporation (%)
1	3	[D]-9	H	14
2		9	D	7
3	5	[D]-9	H	30
4		9	D	32
5	7	[D]-9	H	34
6		9	D	46
7	9	[D]-9	H	39
8		9	D	61
9	11	[D]-9	H	45
10		9	D	67

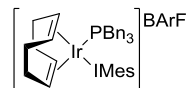


Graph S6. Rate study to determine the kinetic isotope effect.

The data points for 3 min were discarded as they could occur within the catalyst activation period. The data points for 11 min were discarded as product inhibition has been observed when the incorporation is >60%. The gradient of the line is proportional to the reaction rate constant. Therefore, the kinetic isotope effect (k_H/k_D) is (7.25 / 2.25) 3.22.

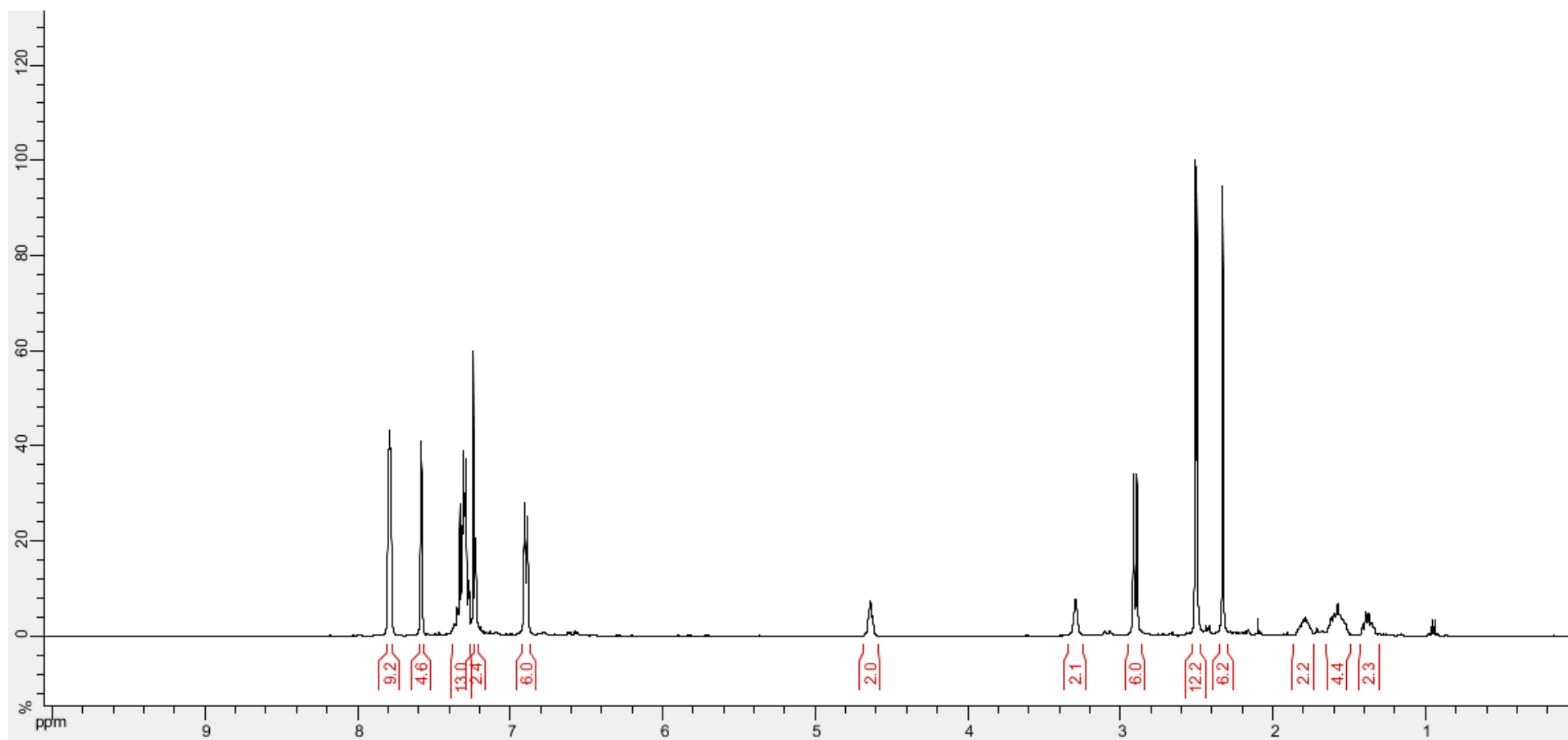
9. Compound Spectra

9.1. Catalyst [(COD)Ir(IMes)(PBn₃)]BARf, 1c.

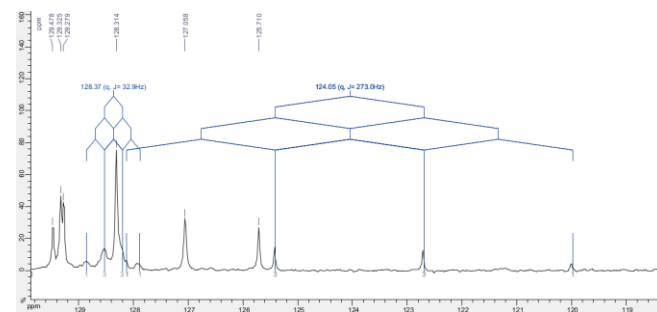
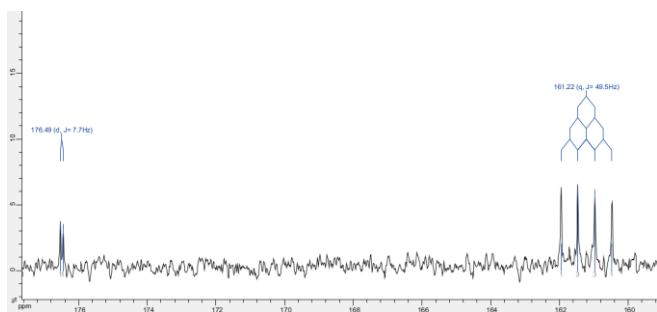
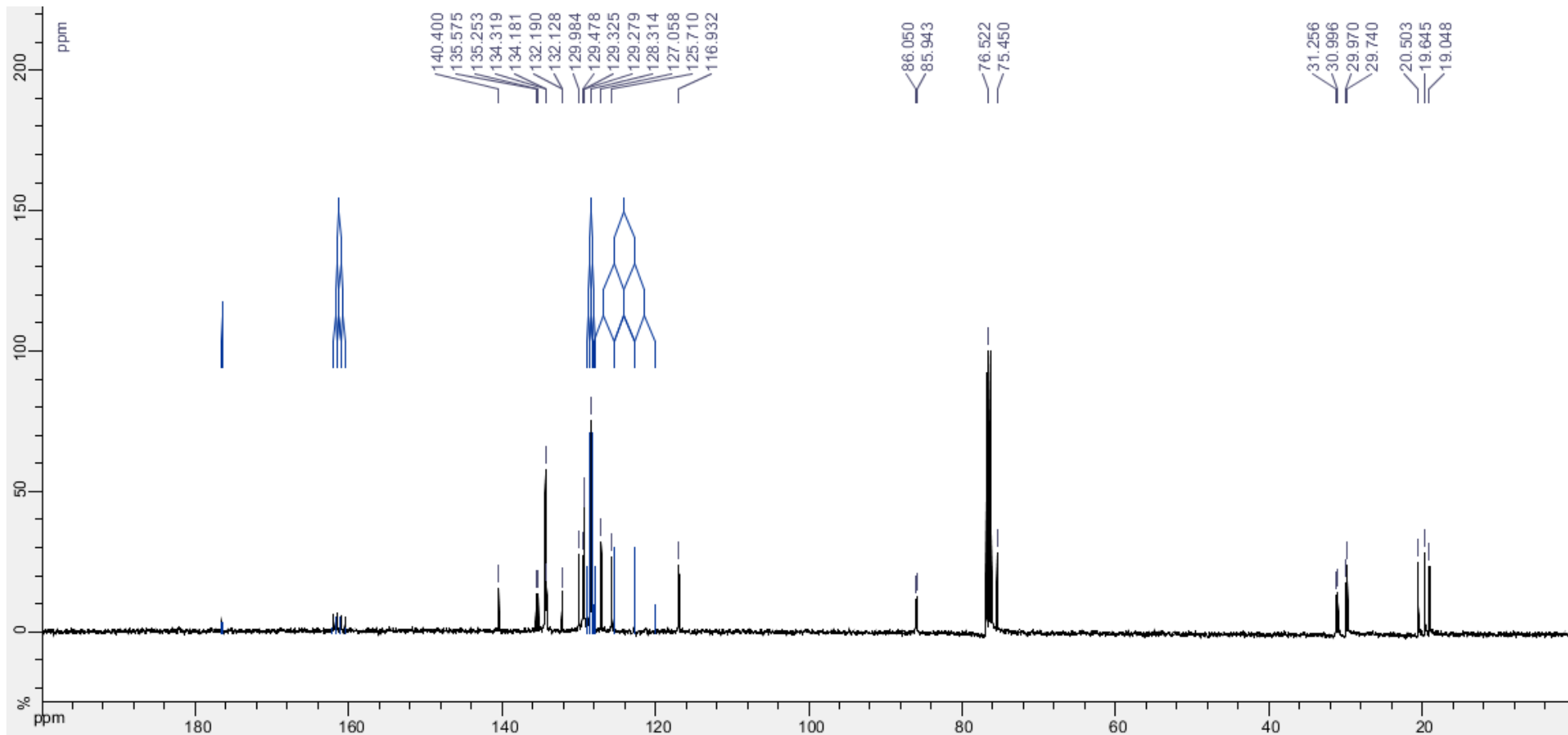


Chemical Formula: C₈₂H₆₉BF₂₄IrN₂P
Molecular Weight: 1772.43

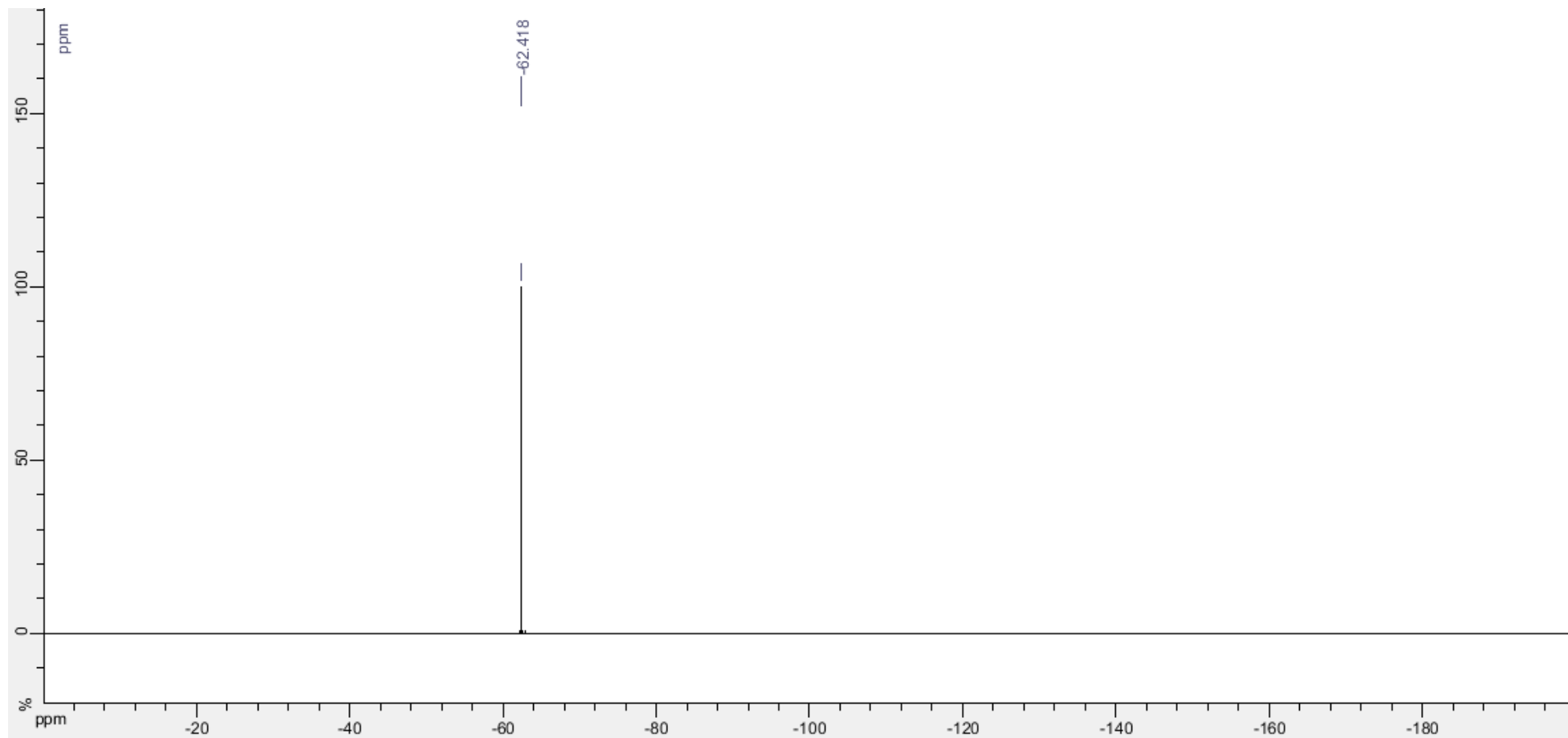
¹H NMR



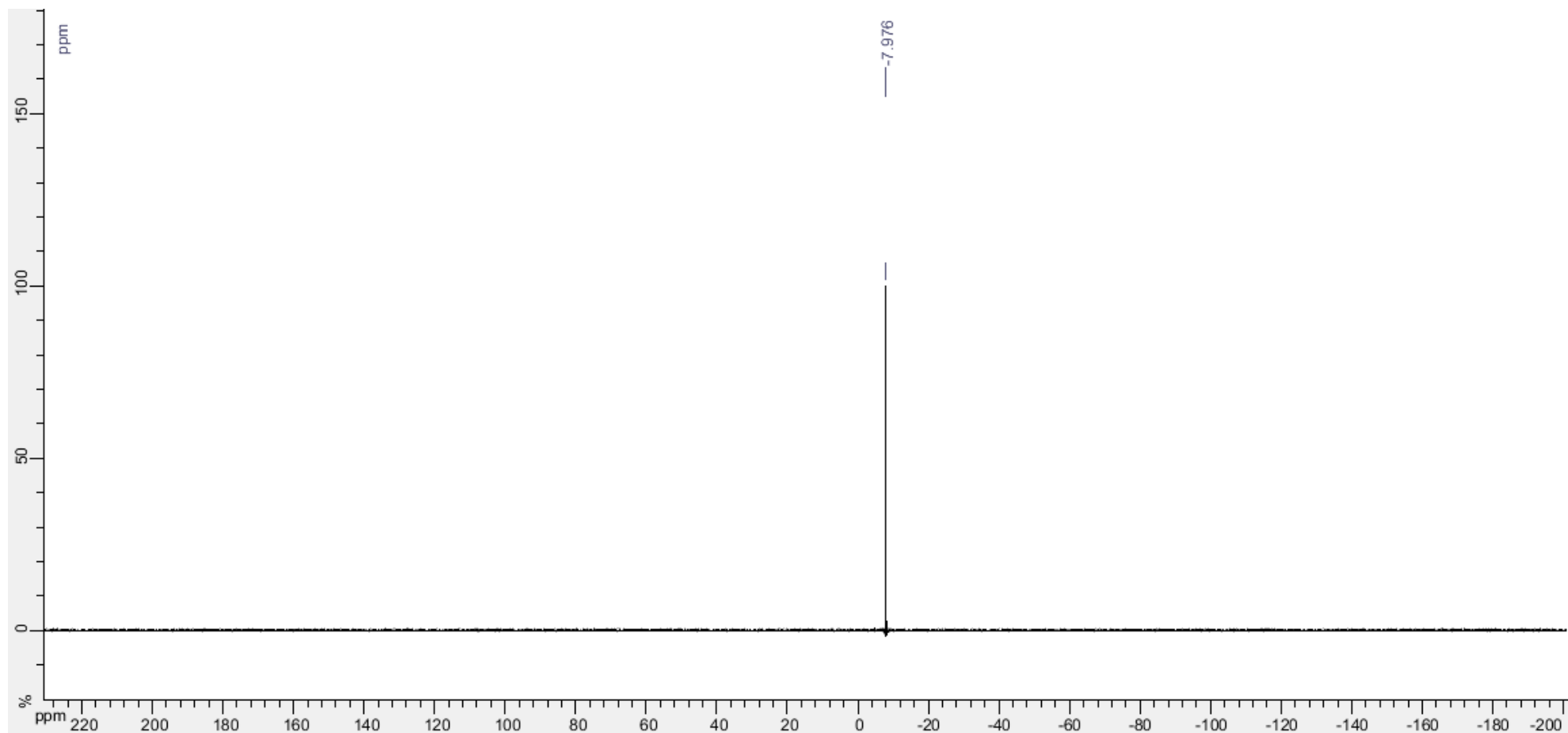
¹³C NMR



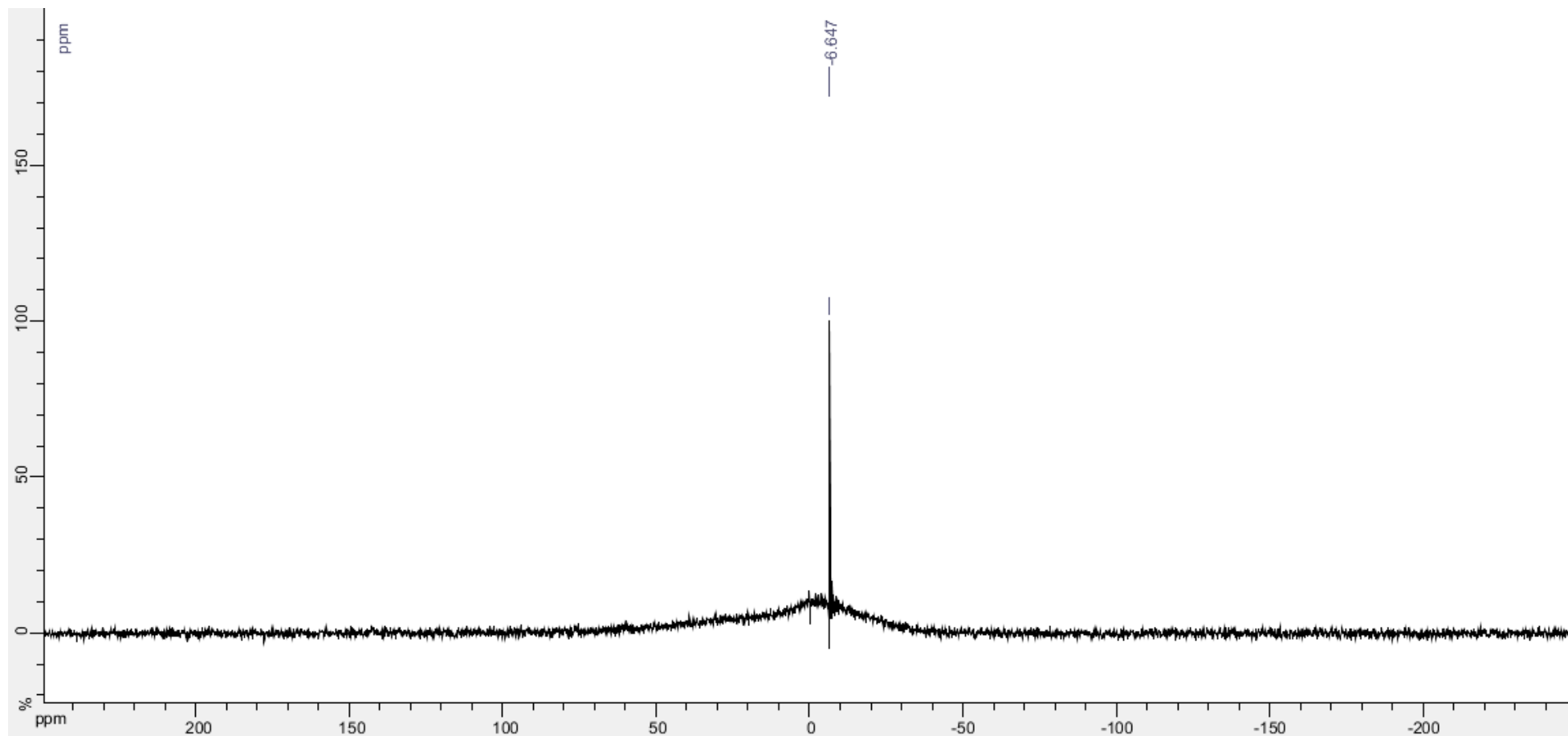
¹⁹F NMR



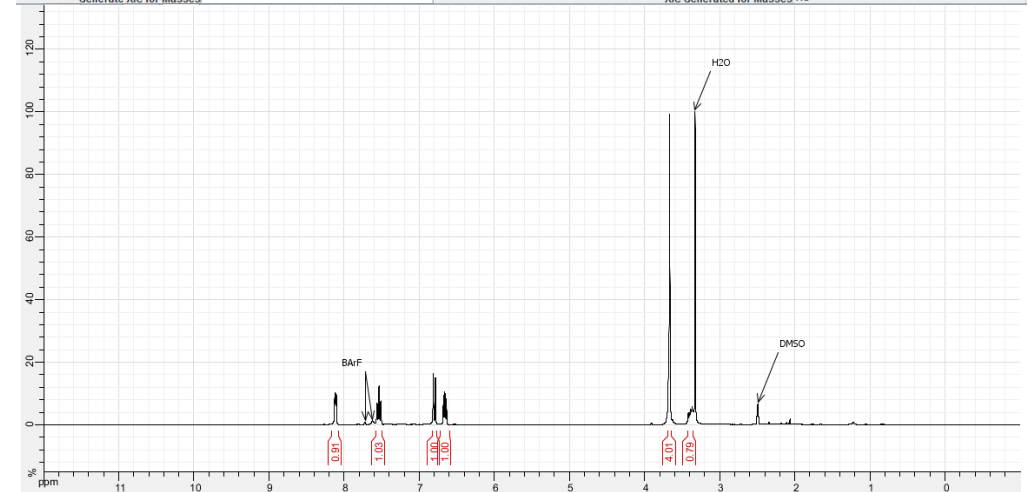
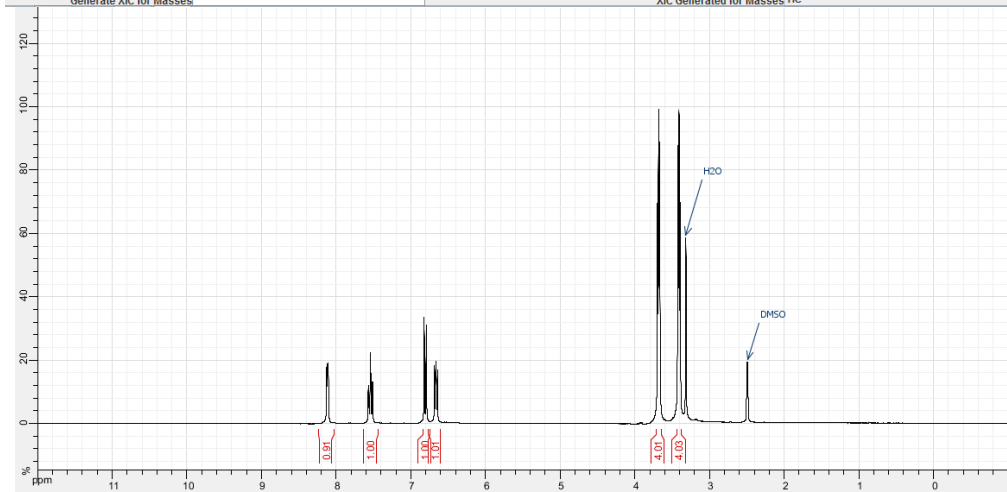
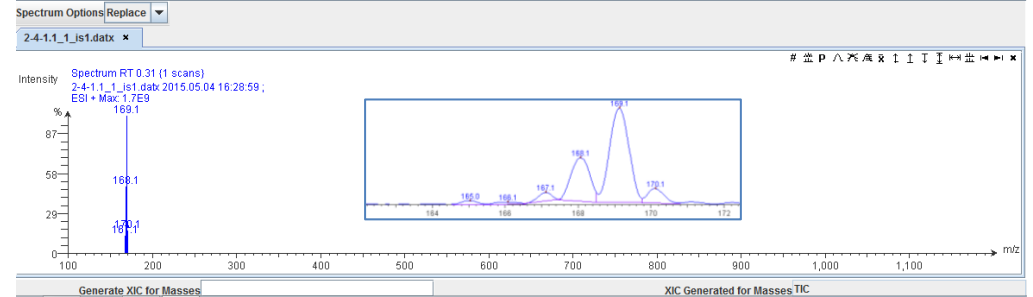
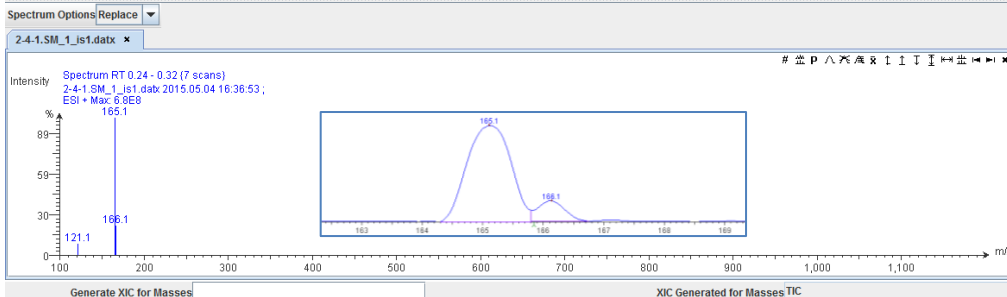
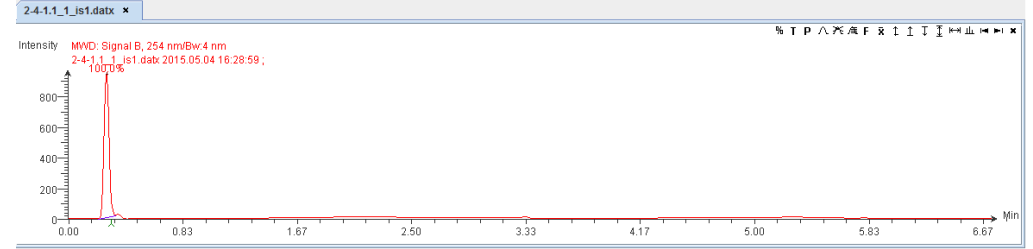
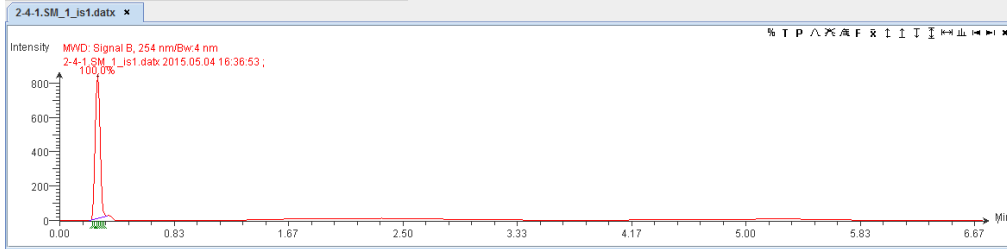
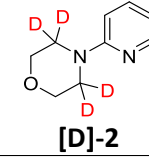
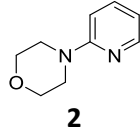
³¹P NMR



¹¹B NMR



9.2. Example LC-MS and NMR data of unlabelled and labelled substrates (2 and [D]-2)



10. References

1. Kennedy, A. R.; Kerr, W. J.; Moir, R.; Reid, M. Anion Effects to Deliver Enhanced Iridium Catalysts for Hydrogen Isotope Exchange Processes. *Org. Biomol. Chem.* **2014**, *12*, 7927-7931.
2. Kerr, W. J.; Mudd, R. J.; Brown, J. A. Iridium(I) N-Heterocyclic Carbene (NHC)/Phosphine Catalysts for Mild and Chemoselective Hydrogenation Processes. *Chem. Eur. J.* **2016**, *22*, 4738-4742.
3. Wüstenberg, B.; Pfaltz, A. Homogeneous Hydrogenation of Tri- and Tetrasubstituted Olefins: Comparison of Iridium-Phosporinoxazoline [Ir-PHOX] Complexes and Crabtree Catalysts with Hexafluorophosphate (PF₆) and Tetrakis[3,5-bis(trifluoromethyl)phenyl]borate (BAR_F) as Counterions. *Adv. Synth. Catal.* **2008**, *350*, 174-178.
4. Wagaw, S.; Buchwald, S. L. The Synthesis of Aminopyridines: A Method Employing Palladium-Catalyzed Carbon–Nitrogen Bond Formation. *J. Org. Chem.* **1996**, *61*, 7240-7241.
5. Boudet, N.; Dubbaka, S. R.; Knochel, P. Oxidative Amination of Cuprated Pyrimidine and Purine Derivatives. *Org. Lett.* **2008**, *10*, 1715-1718.
6. Li, G.; Jia, C.; Sun, K.; Lv, Y.; Zhao, F.; Zhou, K.; Wu, H. Copper(II)-Catalyzed Electrophilic Amination of Quinolone N-Oxides with O-Benzoyl Hydroxylamines. *Org. Biomol. Chem.* **2015**, *13*, 3207-3210.
7. Roiban, G.-D.; Mehler, G.; Reetz, M. T. Palladium-Catalysed Amination of Aryl- and Heteroaryl Halides Using tert-Butyl Tetraisopropylphosphorodiamidite as an Easily Accessible and Air-Stable Ligand. *Eur. J. Org. Chem.* **2014**, *2014*, 2070-2076.
8. Gulevskaya, A. V.; Maes, B. U. W.; Meyers, C.; Herrebout, W. A.; van der Veken, B. J. C–N Bond Formation by the Oxidative Alkylamination of Azines: Comparison of AgPy₂MnO₄ versus KMnO₄ as Oxidant. *Eur. J. Org. Chem.* **2006**, *2006*, 5305-5314.
9. Masashiro, K.; William, H. N.; Naoki, T.; Hiroshi, B.; Yasuhiko, K.; Nobuhiro, I. Fused Quinoline Derivative and Use Thereof. WO2005105802 (A1), November 10, 2005.
10. Romanens, A.; Bélanger, G. Preparation of Conformationally Restricted β^{2,2}- and β^{2,2,3}-Amino Esters and Derivatives Containing an All-Carbon Quaternary Center. *Org. Lett.* **2015**, *17*, 322-325.
11. Compound commercially available from Fluorochem.
12. Compound commercially available from Fluorochem.
13. Katamreddy, S. R.; Carpenter, A. J.; Ammala, C. E.; Boros, E. E.; Brashear, R. L.; Briscoe, C. P.; Bullard, S. R.; Caldwell, R. D.; Conlee, C. R.; Croom, D. K.; Hart, S. M.; Heyer, D. O.; Johnson, P. R.; Kashatus, J. A.; Minick, D. J.; Peckham, G. E.; Ross, S. A.; Roller, S. G.; Samano, V. A.; Sauls, H. R.; Tadepalli, S. M.; Thompson, J. B.; Xu, Y.; Way, J. M. Discovery of 6,7-Dihydro-5H-pyrrolo[2,3-a]pyrimidines as Orally Available G Protein-Coupled Receptor 119 Agonists. *J. Med. Chem.* **2012**, *55*, 10972-10994.
14. Takayama, T.; Shibata, T.; Shiozawa, F.; Kawabe, K.; Shimizu, Y.; Hamada, M.; Hiratate, A.; Takahashi, M.; Ushiyama, F.; Oi, T.; Shirasaki, Y.; Matsuda, D.; Koizumi, C.; Kato, S. Partially Saturated Nitrogen-Containing Heterocyclic Compound. EP2881384 (A1), June 10, 2015.
15. Johnson, P. S.; Ryckmans, T.; Bryans, J.; Beal, D. M.; Dack, K. N.; Feeder, N.; Harrison, A.; Lewis, M.; Mason, H. J.; Mills, J.; Newman, J.; Pasquinet, C.; Rawson, D. J.; Roberts, L. R.; Russell, R.; Spark, D.; Stobie, A.; Underwood, T. J.; Ward, R.; Wheeler, S. Discovery Of PF-184563, a Potent and Selective V1a Antagonist for the Treatment of Dysmenorrhoea. The Influence of Compound Flexibility on Microsomal Stability. *Bioorg. Med. Chem. Lett.* **2011**, *21*, 5684-5687.
16. The compound was obtained from a commercial supplier (Enamine).
17. Bouchon, A.; Diedrichs, N.; Hermann, A.; Lustig, K.; Meier, H.; Pernerstorfer, J.; Reissmüller, E.; de Vry, J.; Mogi, M.; Urbahns, K.; Yura, T.; Jishima, H.; Tajimi, M.; Yamamoto, N.; Yuasa, H.; Gupta, J.; Tsukimi, Y.; Hayashi, F. Tetrahydro-Naphthalene and Urea Derivatives. WO2005040119 (A1), May 6, 2005.
18. Brenner, E.; Schneider, R.; Fort, Y. Nickel-catalysed selective N-arylation or N,N'-diarylation of secondary diamines. *Tetrahedron* **2002**, *58*, 6913-6924.
19. Keenan, M.; Chaplin, J. H.; Alexander, P. W.; Abbot, M. J.; Best, W. M.; Khong, A.; Botero, A.; Perez, C.; Cornwall, S.; Thompson, R. A.; White, K. L.; Shackelford, D. M.; Koltun, M.; Chiu, F. C. K.; Morizzi, J.; Ryan,

- E.; Campbell, M.; von Geldern, T. W.; Scandale, I.; Chatelain, E.; Charman, S. A. Nickel-catalysed selective N-arylation or N,N'-diarylation of secondary diamines. *J. Med. Chem.* **2013**, *56*, 10158-10170.
20. Zimmermann, H.; Bruckner, D.; Henninger, K.; Rosentreter, U.; Hendrox, M.; Keldenich, J.; Land, D.; Radke, M.; Palsen, D.; Kern, A. Heterocyclamid-Substituierte Imidazole. WO2006089664 (A2), August 31, 2006.
21. Thurkauf, A. The synthesis of tritiated 2-phenyl-4-[4-(2-pyrimidyl)piperazinyl]methylimidazole ([³H] NGD 94-1), a ligand selective for the dopamine D₄ receptor subtype. *J. Labelled Compd. Radiopharm.* **1997**, *39*, 123-128.
22. Verma, S. K.; Acharya, B. N.; Kaushik, M. P. Chemospecific and Ligand Free CuI Catalysed Heterogeneous N-Arylation of Amines with Diheteroaryl Halides at Room Temperature. *Org. Biomol. Chem.* **2011**, *9*, 1324-1327.
23. Compound commercially available from Apollo Scientific.
24. Coburn, C. A.; Maletic, M.; Soll, R.; Li, C.; Luo, Y.; Qi, Z. Sulfonamide Derivatives and Methods of Use Thereof for Improving the Pharmacokinetics of a Drug. WO2014000178 (A1), January 3, 2014.
25. Heng, R.; Koch, G.; Schlapbach, A.; Seiler, M. P. Pyrrole Derivatives Useful for the Treatment of Cytokine-Mediated Diseases. WO2008034600 (A1), March 27, 2008.
26. Compound commercially available from Fluorochem.
27. Ueno, H.; Yamamoto, T.; Takashita, R.; Yokohama, R.; Sugiura, T.; Kageyama, S.; Ando, A.; Eda, H.; Eviryanti, A.; Miyazawa, T.; Kirihaara, A.; Tanabe, I.; Nakamura, T.; Noguchi, M.; Shuto, M.; Sugiki, M.; Dohi, M. Sulfonamide Derivative and Medicinal Use Thereof. US2015051395 (A1), February 19, 2015.
28. Compound commercially available from TCI.
29. Wang, D.; Kuang, D.; Zhang, F.; Yang, C.; Zhu, X. Room-Temperature Copper-Catalyzed Arylation of Dimethylamine and Methylamine in Neat Water. *Adv. Synth. Catal.* **2015**, *357*, 714-718.
30. Gowrisankar, S.; Neumann, H.; Beller, M. A Convenient and Practical Synthesis of Anisoles and Deuterated Anisoles by Palladium-Catalyzed Coupling Reactions of Aryl Bromides and Chlorides. *Chem. Eur. J.* **2012**, *18*, 2498-2502.
31. Yuan, Y.; Zaidi, S. A.; Elbegdorj, O.; Aschenbach, L. C. K.; Li, G.; Stevens, D. L.; Scoggins, K. L.; Dewey, W. L.; Selley, D. E.; Zhang, Y. Design, Synthesis, and Biological Evaluation of 14-Heteroaromatic-Substituted Naltrexone Derivatives: Pharmacological Profile Switch from Mu Opioid Receptor Selectivity to Mu/Kappa Opioid Receptor Dual Selectivity. *J. Med. Chem.* **2013**, *56*, 9156-9169.
32. Shen, Z.-L.; Goh, K. K. K.; Wong, C. H. A.; Yang, Y.-S.; Lai, Y.-C.; Cheong, H.-L.; Loh, T.-P. Direct Synthesis of Ester-Containing Indium Homoenate and its Application in Palladium-Catalyzed Cross-Coupling with Aryl Halide. *Chem. Commun.* **2011**, *47*, 4778-4780.
33. Kemperman, G. J. A Method for the Preparation of an Enantiomerically Pure Benzazepine. WO2008125577 (A1), October 23, 2008.
34. Migliaccio, G. P.; Byrn, S. R. Comparisons of Rotamer Populations of Nialamide, Azaperone, and Chloroquine in Solid State and in Solution. *J. Pharm. Sci.* **1981**, *70*, 284-287.
35. Martins, I. L.; Miranda, J. P.; Oliveira, N. G.; Fernandes, A. S.; Gonçalves, S.; Atunes, A. M. M. Synthesis and Biological Activity of 6-Selenocaffeine: Potential Modulator of Chemotherapeutic Drugs in Breast Cancer Cells. *Molecules* **2013**, *18*, 5251-5264.